3D BODY SHAPE CLUSTERING BY PARTICLE SWARM OPTIMIZATION

BY

PORNTHEP SARAKON

A THESIS SUBMITTED IN PARTIAL FULFILLMENT OF
THE REQUIREMENTS FOR THE DEGREE OF MASTER OF
ENGINEERING (INFORMATION AND COMMUNICATION
TECHNOLOGY FOR EMBEDDED SYSTEMS)
SIRINDHORN INTERNATIONAL INSTITUTE OF TECHNOLOGY
THAMMASAT UNIVERSITY
ACADEMIC YEAR 2016

3D BODY SHAPE CLUSTERING BY PARTICLE SWARM OPTIMIZATION

BY

PORNTHEP SARAKON

A THESIS SUBMITTED IN PARTIAL FULFILLMENT OF
THE REQUIREMENTS FOR THE DEGREE OF MASTER OF
ENGINEERING (INFORMATION AND COMMUNICATION
TECHNOLOGY FOR EMBEDDED SYSTEMS)
SIRINDHORN INTERNATIONAL INSTITUTE OF TECHNOLOGY
THAMMASAT UNIVERSITY
ACADEMIC YEAR 2016

3D BODY SHAPE CLUSTERING BY PARTICLE SWARM OPTIMIZATION

A Thesis Presented

By

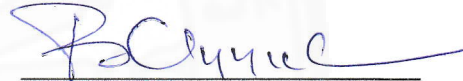PORNTHEP SARAKON

Submitted to

Sirindhorn International Institute of Technology

Thammasat University

In partial fulfillment of the requirements for the degree of

MASTER OF ENGINEERING (INFORMATION AND COMMUNICATION

TECHNOLOGY FOR EMBEDDED SYSTEMS)

Approved as to style and content by

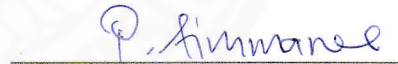Advisor and Chairperson of Thesis Committee _____

(Assoc. Prof. Dr. Bunyarit Uyyanonvara)

Co-Advisor _____

(Dr. Supiya Charoensiriwath)

Committee Member and
Chairperson of Examination Committee _____

(Asst. Prof. Dr. Pakinee Aimmanee)

Committee Member _____

(Assoc. Prof. Dr. Hirohiko Kaneko)

JUNE 2017

i

Abstract

3D BODY SHAPE CLUSTERING BY PARTICLE SWARM OPTIMIZATION

by

PORNTHEP SARAKON

Bachelor of Engineering in Biomedical Engineering, Srinakarinwirot University, 2015
Master of Engineering in Information and Communication Technology for Embedded Systems, Sirindorn International Institute of Technology, Thammasat University, 2017

Human body shape plays an important role in many industries, especially in Healthcare. We have seen changes in the body size and shape of the Thai population from the data collected through national sizing surveys over two decades. These changes can also indicate the trend of national health status. In this thesis, we propose a human body analysis algorithm and a human body shape clustering algorithm.

First, the human body analysis algorithm, called as data acquisition part, is created to avoid a dependence on software of scanner. This part consists of three steps. The first step is a plane adjustment. It is used to set 3D body data into the same format. Moreover, a body segmentation step separates torso data without other. The final step is body landmark detection and measurement in order to prepare these data for the human body shape clustering part.

Second, the human body shape clustering algorithm is designed to solve problem of need of training, model recognizing and fixing a number of the final group. This part consists of three steps. The first step is a fitness function creation. We create it from the combination between volumetric and anthropological difference. Furthermore, the preprocessing of PSO is a method that looks for the best parameters of PSO for the best performance. The final step is the human body shape clustering based on PSO, which is used to group body shapes according to each body size.

In sum, in the data acquisition part, the accuracy of it is high enough to use as input data for second part. The accuracy of bust, hip and small of back waist detection are 100.00%, 98.89% and 96.67 % respectively. In the human body shape clustering part, the best result is provided by threshold at 0.3 and the ratio at [0.4: 0.6] of volumetric overlap to euclidean distance fitness function condition. Its success rate is 93.33% as well as average iteration and time is minimum of all conditions. Results are then compared with those obtained from k-means clustering and the identified shapes from the Female Figure Identification Technique. The results show that those of PSO clustering can be identified body shape more than those of k-mean algorithm did.

Keywords: Particle swarm optimization (PSO), k-means algorithm, clustering

Acknowledgements

There are many people that I would like to thank for a huge variety of reasons.

Firstly, I would like to express my deep and sincere gratitude to my supervisors, Dr. Supiya Charoensiriwath and Assoc. Prof. Dr. Bunyarit Uyyanonvara, for their continual support and guidance throughout the course of my Masters. Their constant encouragement and enthusiasm have helped me get through difficult periods and keep me on course. Without their input and tireless efforts, this journey would have been far less tolerable.

I would like to thank my thesis committees, Asst. Prof. Dr. Pakinee Aimmanee and Assoc. Prof. Hirohiko Kaneko, for providing me with their encouragement, insightful comments, and interesting questions. They always help me to improve my research work.

I am particularly thankful to all researchers at Healthy and Lifestyle Monitoring Laboratory, National Electronics and Computer Technology Center, Thailand for their suggestion, encouragement and the best working place for this research.

A special big thank you to my friends, Siriporn Pattamaset and Setthawut Kiattisaksophon, for dragging me away from my work when I needed a break, for all night that I can stop my work.

Finally, my heartfelt thanks to my family, without whom it would have been impossible to finish this thesis. A huge thank you to my parents, Parinya and Anoporn

Sarakon, for their unconditional love, support and endless encouragement. This work is dedicated to them.

Table of Contents

List of Figures

List of Tables

Chapter 1

Introduction

Good health is important in human life. Because it is one of the happiest factors of those, everyone is interested in it. For example, people always exercise and have healthy food in order to have good health as well as they have an annual medical check-up so as to track their health change. Health changing tracking which has several ways depends on criteria of measurement, such as change of weight and body shape.

This thesis focuses on change of body shape. Due to body shape that has changed, it can well indicate everyone's trend of health having either better or worse. It can be used as health indicator in order to prevent sickness from disease. For example, obesity causes other diseases, such as hypertension, diabetes and heart disease.

Therefore, human body analysis and clustering is a very important topic. We have seen changes in the body shape of the Thai population from the data collected through national sizing surveys over the past 20 years. Moreover, Thai people body shape has been divided by human body shape expert. Because of this reason, Thai body shape database updating must spend so much time and causes to occur delay. Creating human body analysis and human body shape clustering system are needed in order to reduce updating time. However, in current, these systems use the national sizing survey information, which consists of body measurements of human that are measured by expert and spend too much time.

Since, the first national sizing survey using a 3D body scanner (SizeThailand) conducted by NECTEC in 2007-2009[1,2], it is now possible to define body shapes in 3D. The 3D body scanner can reduce body-measuring time, but in the present, it has a limitation that is a fixation between an analysis system (software) and scanner in each manufacturer. When going to display measurement with 3D body data, we must put data into it. However, there is no combination between analysis and clustering in a system. Therefore, creating algorithm for analysis and division into groups based on 3D data is essentially important to reduce the time and work method. This thesis is concerned with human body analysis and human body shape clustering system as to be discussed below.

1.1 Human Body Shape Analysis System

Human body analysis system is a system used for measuring body measurements from 3D body data after 3D scanner collects this data, most of which is coordinated points in Cartesian coordinate system. The human body analysis system can scale body measurements, such as bust, waist and hip circumference or their high position. In currently, this system has some limitations that are manufacturer specifications between it (software) and 3D scanner (hardware). Due to capturing and collecting format of different manufacturers, they are usually used by the clustering system in order to extract body measurement.

1

1.2 Human Body Shape Clustering System

Human body shape clustering system is a system used for dividing or assembling human body shape. It divides different body shapes and assemble same ones in order to collect systematically with using body measurement data that are extracted by the human body analysis system. Most clustering systems identify the body shape first and then collect to group. Additionally, this system has another method that defines body shape types or number of those first and then divides for grouping. According to previous method, it causes problems for clustering. For example, population-changing problem usually occurs when population increases or decreases as well as some data cannot identify body shape because they are not defined shapes.

1.3 Motivation

In recent years, technologies that are computer vision and swarm intelligence are widely used for diverse purposes. Due to their working speed and accuracy, they become more popular and popular in human body shape clustering as well. 3D scanner, which is one of the computer vision technologies, is used to reduce time of collecting data. Because of fixation between human body analysis system and scanner (hardware), we would like to create the analysis system, which can apply to 3D body data without no need to fix the scanner. Moreover, currently, human body shape clustering system has limitations that are the need of having shape models so as to be defined template first and then compare with data input as well as collect data to its group. Unless there is a template, it cannot work. According to this problem, we would like to solve it by using Particle Swarm Optimization (PSO), most of which are used for solving computational time and finding solution without training. For this reason, the PSO is appropriate with solving this problem as well as improving performance on working speed. Therefore, if we combine human body analysis and human body shape clustering together, the problems of long working hours, the problem in need of extracted data from 3D scanner and the problem of the need for template will be solved.

1.4 Objective

The objectives of this thesis research are as follows:
- Create a 3D human body data acquisition that instead of depending on extracted data from software included in 3D scanner.
- Create a 3D human body shape clustering algorithm that can be used with changeable population and work without the need to fix the number of the final body shape clusters.

1.5 Thesis Outline

In this thesis, there are totally five chapters including Chapter 1, which is Introduction. Chapter 2 discusses the reviews of related work divided into two parts: related works of human body analysis and human body shape clustering. The research work of human body analysis part is shown in Chapter 3 divided into two parts, which are proposed methodology and experimental results. Similarly, Chapter 4 describes the proposed methodology and experimental results of human body shape clustering. Chapter 5 gives conclusion and future works for both systems.

Chapter 2

Literature Review

Due to benefit of human body analysis and human body shape clustering algorithm, there are studies and developments in many industries, such as fashion, computer vision and healthcare industry. In the healthcare industry, these systems are used to analyze the tendency of health in personal and national level by computer vision and intelligent computational technology. However, the human body shape clustering has a main problem that is dependence on extracted data from 3D scanner, model need and a need to fix the number of final body shape clusters. This chapter discusses previous works of human body analysis and human body shape clustering related to this thesis. Some methods of the previous works were adopted and modified in this research work for better performance of the research result.

2.1 Literature related to human body analysis

2.1.1 Related works of Human body analysis

In recent year, most human body analysis systems are usually included in the 3D body scanner. These systems were studied by researcher for twenty years. For example, $[TC]^2[3]$, which is developed by $[TC]^2$ labs, is 3D body scanner including human body analysis software. Due to speed of data collecting and body measuring, they are more popular in nowadays as well as are used for nation sizing survey in many counties, such as United Kingdom having SizeUK[4], the United State has SizeUSA [5] or $[TC]^2$, South Korea having Size KOREA[6], Japan having Size-JPN[7] and Thailand having SizeThailand[8]. However, depending on extracted data by 3D scanner is not our desire. We look for new human body analysis method, which does not depend on the scanner, and find that there is a 3D head segmentation study in [9]. A method is plane creation between occipital head and pharynx after detecting both of them. Moreover, there is 3D human body detection study, such as bust, waist and hip in [10] as well as we adopt and modified it in order to increase performance of body detection, such as bust, small of back waist, maximum waist, minimum waist and hip in [11]. According to previous works, we can divide the human body analysis methods to 4 methods as follows:

1. Body scanning: this step is 3D object scanning that covert to coordinate in Cartesian systems.

2. Data acquisition: this step, which is important, consists of body plane adjustment, rearranging body data and body height normalization. Because 3D body data is collected by different 3D scanner, the data have several formats. Therefore, the data should adjust to the same format.

3. Body measurement detection: a computer vision usually plays a role in this step because the 3D body data is coordinate, like a 3D object.

4

4. Body measurements measuring: this step is usually used to extract the body measurements.

This thesis studied and modified only 3 last steps because we aim to solve the dependence problem on extracted data from 3D scanner.

2.1.2 Related works of head segmentation Algorithm

A head segmentation algorithm is a method that is used by [9] in the human body analysis. It can adjust the data plane, rearrange data as well as segment head and torso data. Furthermore, this method is created in order to use with 3D body data, which is explained as follows:

$$A = \frac{1}{N} \sum_{i=1}^{N} (X_i - \mu)(X_i - \mu)^T$$

(2.1)

where $X_i = [x_i; y_i; z_i]$ is coordinate of a point in 3D space, $\mu = [\mu_x; \mu_y; \mu_z]$ is mean coordinate, N is number of points.

By using Eigenvalue and Eigenvector for Eq. (2.1), 3D body data, being coordinate in Cartesian systems, is detected distribution axis by three values of eigenvalue(λ): $\lambda_1, \lambda_2, \lambda_3$ and three directions of eigenvector (e): e_1, e_2, e_3 are derived so as to specify body axis. For example, vertical axis is height axis, horizontal axis is width axis and anterior-posterior axis is depth axis, which are shown as red, green and blue vector in Fig. 2.1. The body axis and body direction identification is explained as follows:

1. In vertical axis detection, because it is a longest axis, it will be identified with maximum distribution axis. On the another hand, a shortest axis identify in order to be anterior-posterior axis. In addition, the other axis is horizontal axis.
2. After we knew all axis, we get 10 percent of sample data each of which are maximum and minimum part in vertical axis in order to identify face direction. Head data have data distribution in horizontal axis less than foot data.
3. The face direction is identified by finger foot direction.
4. Finally, we knew both axis and direction of the 3D body data and then rotate as well as normalize to same way.

5
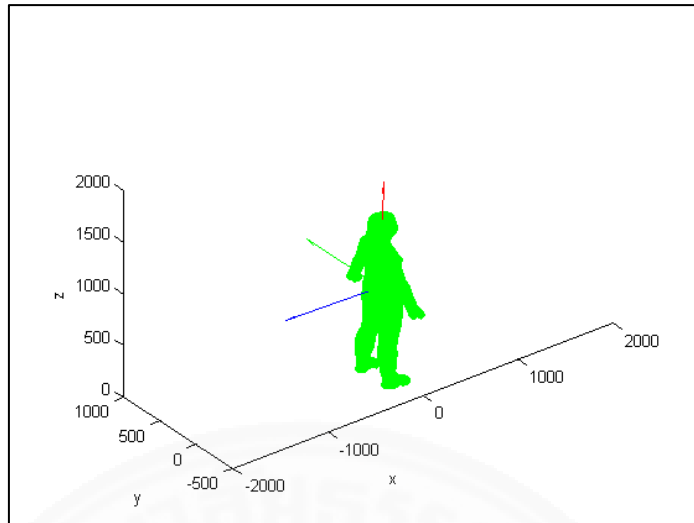
Fig. 2.1 Head Segmentation Algorithm [9]

2.2 Literature related to human body shape clustering

2.2.1 Related works of human body shape clustering

There are human body shape clustering systems, which are studied in diverse ways. Because of their work principles, they are divided into 2 types that are need of training and no need of training.

First, grouping method by training is well known as machine learning technology. Because learning ability of this technology is fast, it is used to solve many problems and body grouping as well. A main method of machine learning in this area is training in human body shape identification. For example, it is trained by conditional training or model recognizing. The conditional training[12,13] is method that spends the shortest time to teach machine learning. However, conditional creator needs to work hard and spends so much time so as to get the best and most suitable conditions for his data. Moreover, model recognizing training[10,13], which is the most popular method in nowadays, is an easy way for who have a good and clear model in order that the machine learning can performantly work. Unless we cannot create suitable condition, have good model or have new shape data, this method cannot work in this case.

Second, grouping method by no training is another one that is equally popular to first method. A k-mean is well known in groups by need of a number of the final group. It is used to divide groups of human body shape as well in [15]. By using body measurements in order to be data in clustering. If you know a suitable number of the final group, k-mean will be the best choice for you. Unless you do not know that number, k-mean will not be a method that you should use and fuzzy clustering based on PSO [16] also. Moreover, other method that do not need to know the number of final group. Firstly, it is hierarchical clustering. Thanks to its advantage, it is used for the human body shape clustering in [17,18,19]. However, it appropriates with few groups only. Another one is particle swarm optimization (PSO), which is a particular type of swarm intelligence. Due to its abilities, which are no need of a number of the

6

final group and support with dynamic population, PSO is used by us to the 3D human body shape clustering in [11,20]. Therefore, PSO is selected by us in order to solve 3D human body shape clustering problems.

2.2.2 Related works of PSO algorithm

Particle swarm optimization (PSO) is population-based evolutionary technique developed by Eberhart R. C. and Kennedy J. [21]. It exhibits self-organization and searches the solution space for optima through iterative procedures. However, it differs in individual itself, each of which called "particle" contains position and velocity (n-dimensional vectors). The velocity responses to position change of particle in order to explore a space of all possible solutions. When particles move around the space, they will find a sample of different solution that come from different locations. Each position have different fitness score according to solution that objective function have. Due to rules that govern processing of swarm, particles swarm continuously around the space in which fittest solution is.

According to The underlying socio-cognitive theory presented in [22], it present that particles are influenced by their best success as the cognitive part and by success of each particle in their neighbors as the social part. Each particle can connect to each other in neighborhood. According to Kennedy's book, Swarm Intelligence [23], the two most common ways, which each particle can connect topologically is The *lbest* (local best) neighborhood and The *gbest* (global best) neifghborhood.

- The *lbest* (local best) neighbourhood

  Each individual's neighborhood consists of itself and its k adjacent neighbors [24]. For example, if we let k equals to two, a ring topology of this neighborhood is shown as Fig. 2.2.
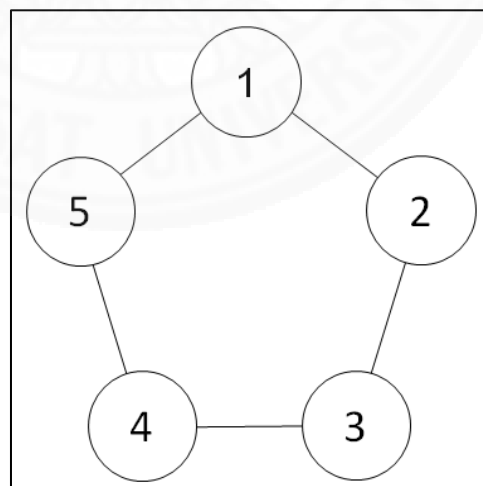
Fig. 2.2 The *lbest* topology where k=2

- The *gbest* (global best) neighbourhood

  All individual in *gbest* neighborhood connect and each particle is influenced by the best performance of any in the entire population [24] as shown in Fig. 2.3.

7
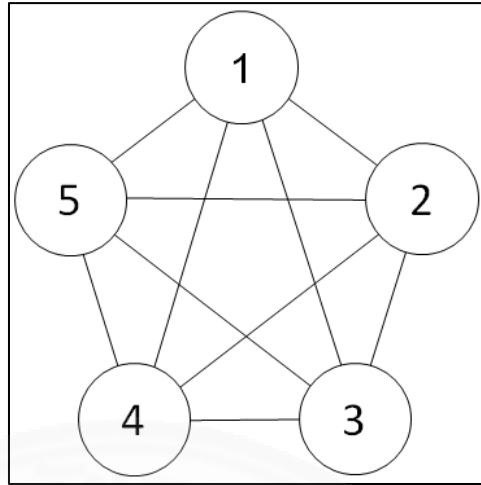
Fig. 2.3 The gbest topology

Therefore, particles' velocity and position are updated as each iteration according to two best positions which are *pbest* (personal best) and *gbest* (or *lbest*, depending on the chosen neighborhood topology). The *pbest* presents particle's previous best position, fitness score of which is stored. The *gbest* or *lbest* present best position that are attained by any member in the swarm (or those are in the particle's *lbest* neighborhood). Fig. 2.4 shows the PSO algorithm that was proposed by Kennedy and Eberhart in [25]. The particle update algorithm used in order to modify particle velocities and positions is governed by these three rules (Eq. (2.1, 2.2 and 2.3)):

$$v_i = wv_i + c_1r_1(x_{pbest,i} - x_i) + c_2r_2(x_{gbest,i} - x_i) \qquad \text{Rule 1(2.1)}$$
$$if(|v_i| > v_{max}) \quad v_i = (v_{max}/|v_i|)v_i \qquad \text{Rule 2(2.2)}$$
$$x_i = x_i + v_i \qquad \text{Rule 3(2.3)}$$

Where x_i is the current position of particle i

x_{pbest} is the best friend position attained by particle i

x_{gbest} is the swarm's global best position

v_i is the velocity of particle i

w is a random inertia weight between 0.5 and 1 [26]

c_1, c_2 and c_3 are spring constants whose values are set to 1.494 [26]

r_1, r_2 and r_3 are random numbers between 0 and 1 [27]

8

INITIALISE the swarm with random initial positions

SET each particle's *pbest* to be the initial position

SET one *pbest* that returns the best fitness score to be the swarm's *gbest*

LOOP

UPDATE velocity of each particle according to Rule1

    CHECK velocity limit according to Rule2

    UPDATE position of each particle according to Rule3

    If the fitness of the new position is better than the particle's *pbest* fitness

        Then REPLACE *pbest* position with the new position

    If the fitness of the particle's *pbest* is better than the swarm's *gbest* fitness

        Then REPLACE *gbest* position with the particle's *pbest* position

UNTIL either the fitness of *gbest* is below a threshold value or the maximum number of iterations is reached

Fig. 2.4 PSO algorithm

A modify PSO [28] was proposed by Supiya Ujjin. She adds another variable called "outsider" which is the position that needs to avoid by using a repelling force. Moreover, she proposed a new rule that is used for update position in order to avoid outsider's position. This rule is added between rule1 (Eq. (2.1)) and rule3 (Eq. 2.2)). Outsider is particle that is neighborhood but does not belong there because fitness score more than threshold defined. Therefore, this modified PSO algorithm is employed in this thesis. The particle dynamics are governed by the following rules, which update particle position and velocities:

$$v_i = wv_i + c_1r_1(x_{pbest,i} - x_i) + c_2r_2(x_{gbest,i} - x_i) \quad \text{Rule 1(2.1)}$$
$$v_i = v_i + f_3c_3r_3(x_{avoid,i} - x_i) \quad \text{Rule 2(2.4)}$$
$$if(|v_i| > v_{max}) \quad v_i = (v_{max}/|v_i|)v_i \quad \text{Rule 3(2.2)}$$
$$x_i = x_i + v_i \quad \text{Rule 4(2.3)}$$

Where x_i is the current position of particle i
    x_{pbest} is the best friend position attained by particle i
    x_{gbest} is the swarm's global best position
    x_{avoid} is the all outsider position attained by particle i
    v_i is the velocity of particle i
    w is a random inertia weight between 0.5 and 1
    c_1, c_2 and c_3 are spring constants whose values are set to 1.494
    r_1, r_2 and r_3 are random numbers between 0 and 1
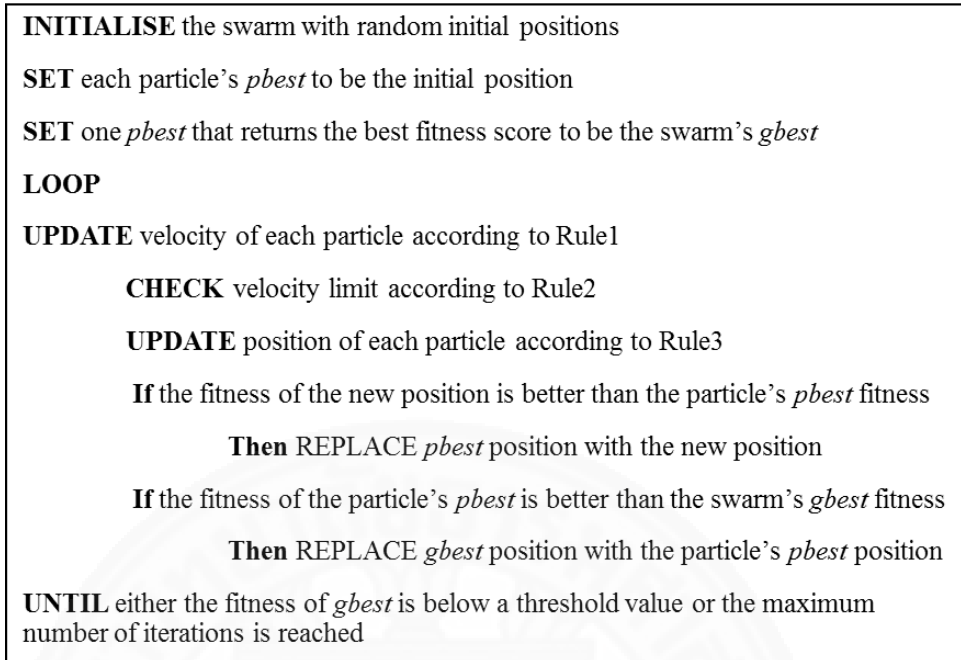 f_3 is the repulsive factor

9

Chapter 3

Human body analysis methodology and experimental result

In this thesis, main methodology consists of 2 parts. A first part is the data acquisition part called human body analysis and the second part is clustering part called human body shape clustering, which is shown in Fig. 3.1. According to human body analysis system described in Chapter 2, most data acquisitions depend on a 3D body scanner because this software system include within the scanner. This is a problem if we want to use 3D body data from different scanners. Therefore, we aim to create an algorithm that does not depend on the scanner in order to prepare 3D body data for clustering part. Moreover, this thesis can be improved by utilizing the related work so that body measurement detection will be increase its accuracy. The 3D body data, which is used in the experiment, is body data in 3 dimensions. It consists of coordinate in Cartesian system that is called texture coordinate without vertex color. This 3D body data captured, using $[TC]^2$, was collected by SizeThailand at nation sizing survey in 2007-2009. Its example is shown as Fig. 3.2. The details of the methodology and results are described in this chapter.
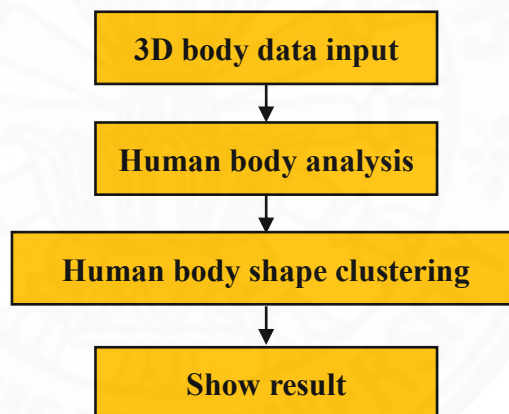
Fig. 3.1 3D Body Shape Clustering by Particle Swarm Optimization flowchart.
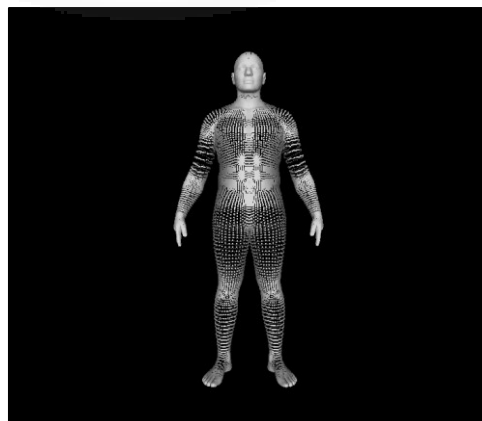
Fig. 3.2 Example of 3D human body data.

3.1 Methodology

Human body analysis methodology consists of 3 sections that are plane adjustment, body segmentation as well as body landmark detection and measurement as shown in Fig. 3.3. First, the purpose of plane adjustment method is a 3D body adjustment, which is the same face direction and position, in the same direction described in section 3.1.1. Moreover, section 3.1.2 describes body segmentation, which is designed to segment used data because we want to use torso data only. The torso data is prepared in order to use for human body shape clustering part described in Chapter 4. Finally, the purpose of body landmark detection and measurement method is body landmarks detection, such as bust, small of back waist, maximum waist, minimum waist and hip, so as to measure and then use for Chapter 4.

```
┌─────────────────────────────────────┐
│         3D body data input          │
└─────────────────────────────────────┘
                  ↓
┌─────────────────────────────────────┐
│          Plane adjustment           │
└─────────────────────────────────────┘
                  ↓
┌─────────────────────────────────────┐
│          Body segmentation          │
└─────────────────────────────────────┘
                  ↓
┌─────────────────────────────────────┐
│  Body landmark detection & measurement │
└─────────────────────────────────────┘
                  ↓
┌─────────────────────────────────────┐
│       Human body shape clustering   │
└─────────────────────────────────────┘
```
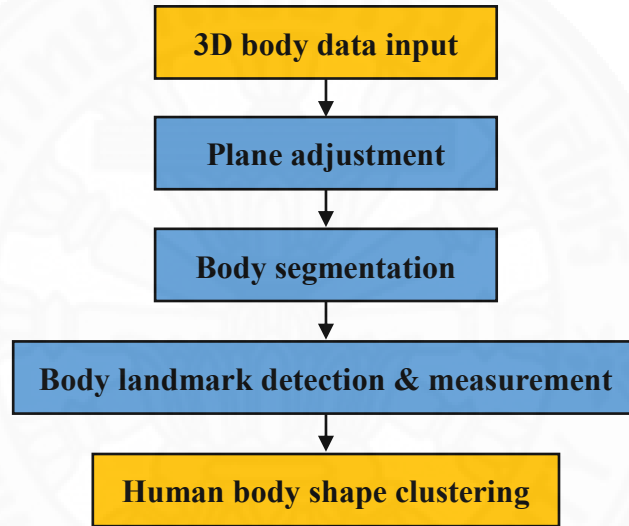
Fig. 3.3 Human body analysis methodology flowchart.

3.1.1 Plane adjustment

This is the first step of the proposed methodology. This thesis modifies body plane adjustment method proposed by [9] in order to adjust 3D body plane in the same direction and position. This technique is based on eigenvector and eigenvalue described in Eq. (3.1).

$$A = \frac{1}{N} \sum_{i=1}^{N} (X_i - \mu)(X_i - \mu)^T$$

(3.1)

where $X_i = [x_i; y_i; z_i]$ is coordinate of a point in 3D space, $\mu = [\mu_x; \mu_y; \mu_z]$ is mean coordinate, N is number of points.

11

By using Eigenvalue and Eigenvector for Eq. (3.1), 3D body data that is coordinate in Cartesian system is identified data distribution by three values of eigenvalue ($\boldsymbol{\lambda}$): $\boldsymbol{\lambda_1, \lambda_2, \lambda_3}$ and three directions of eigenvector ($\boldsymbol{e}$): $\boldsymbol{e_1, e_2, e_3}$ in order to identify body axis. The body axises consist of vertical axis, horizontal axis and anterior-posterior axis. If they are sort by length from longest to shortest, vertical axis will be the longest axis and anterior-posterior axis will be the shortest axis. Fig. 3.4 (b) shows red, green and blue vector that are vertical, horizontal and anterior-posterior axis, respectively. The method of plane adjustment is described as follows:

1. When identifying a 3D body data by Eq. (3.1), we will get Eigenvalue and Eigenvector, which can explain what direction and scale of distribution-axises of 3D data is.
2. Axis identification is described by Chapter 2. The longest axis that has maximum eigenvalue is vertical axis, the shortest axis that has minimum eigenvalue is anterior-posterior axis and the other one is horizontal axis, all of which is shown in Fig. 3.4 (b).
3. In order to identify body-position direction, we use sample of 3D body data in vertical axis that have maximum and minimum value as shown in Fig. 3.4 (c). Moreover, we measure their distributions to check data that have eigenvalue in horizontal axis less than another as well as then define it as head direction and other as foot direction.
4. Furthermore, so as to identify face and back direction of the 3D body data, we check finger foot direction from foot data as shown in Fig. 3.4 (d).
5. Finally, after we knew all of axises, directions and size of the 3D body data, it is rotated by Eq. (3.3, 3.4, 3.5) and normalize body size. An output is shown in Fig. 3.4 (f) and examples of results are shown in Table 3.1.

$$A * Rotation = B$$

$$(3.2)$$

$$RotationX = \begin{bmatrix} 1 & 0 & 0 \\ 0 & \cos(\theta) & -\sin(\theta) \\ 0 & \sin(\theta) & \cos(\theta) \end{bmatrix}$$

$$(3.3)$$

$$RotationY = \begin{bmatrix} \cos(\theta) & 0 & \sin(\theta) \\ 0 & 1 & 0 \\ -\sin(\theta) & 0 & \cos(\theta) \end{bmatrix}$$

$$(3.4)$$

$$RotationZ = \begin{bmatrix} \cos(\theta) & -\sin(\theta) & 0 \\ \sin(\theta) & \cos(\theta) & 0 \\ 0 & 0 & 1 \end{bmatrix}$$

$$(3.5)$$

where $A = [x_i; y_i; z_i]$ is input that is coordinate of a point in 3D space, $B = [x_i; y_i; z_i]$ is input that is coordinate of a point in 3D space, $Rotation$ is rotation matrix.
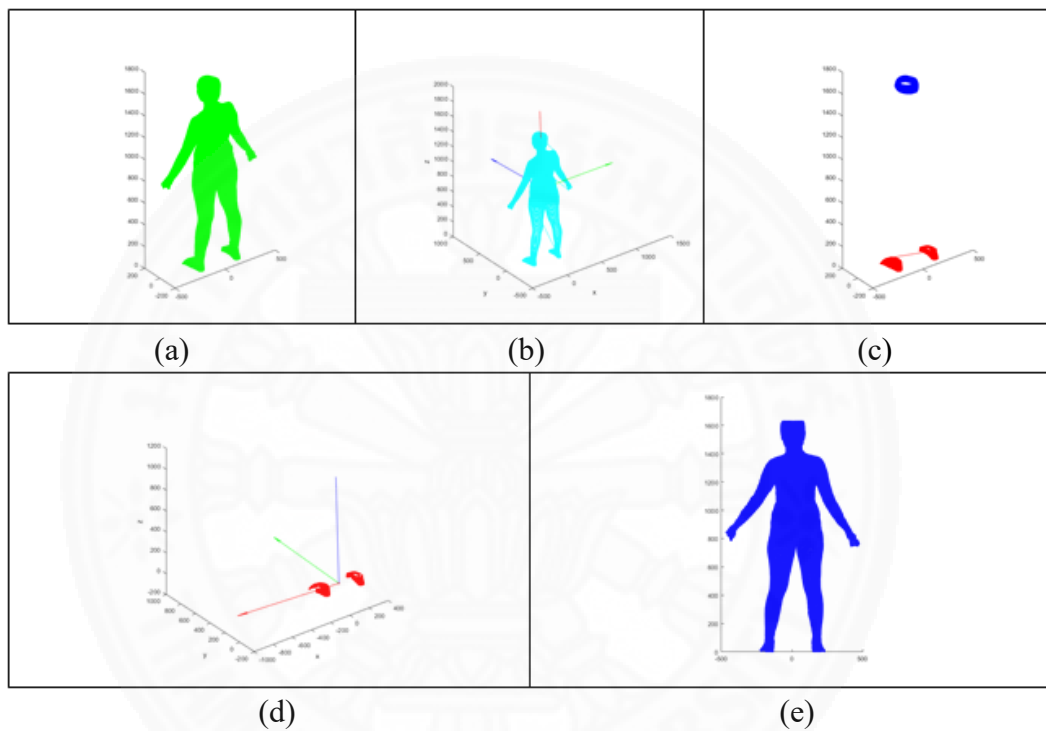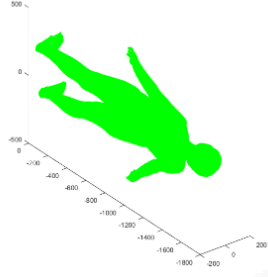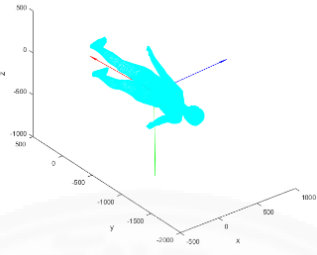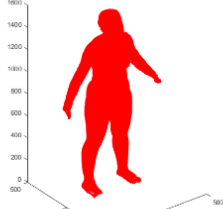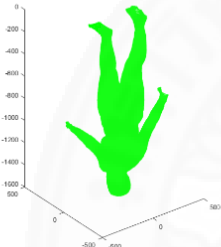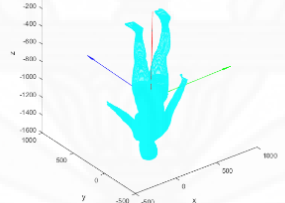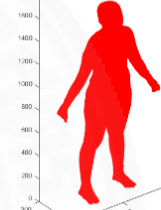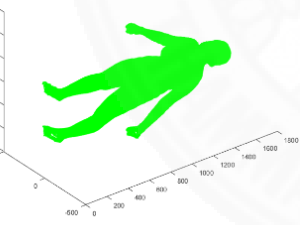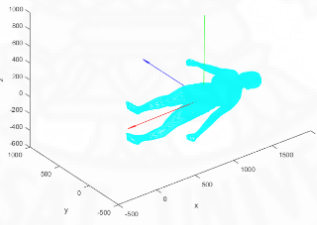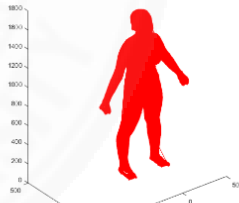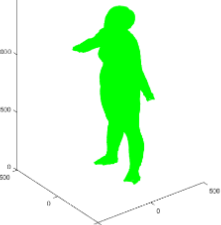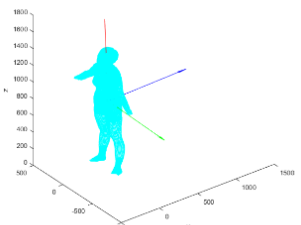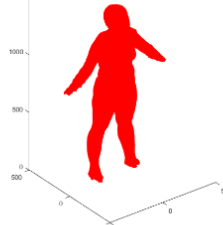
Fig. 3.4 Plane adjustment method start from (a) input data, (b) eigenvector and eigenvalue identification, (c) head direction identification, (d) finger foot direction checking, and (e) result of plane adjustment method.

13

Table 3.1 Examples of plane adjustment results

Input data	plane adjustment methodology	Result of plane adjustment

3.1.2 Body segmentation

Body torso is important data for body shape clustering. The purpose of this method is data segmentation that is torso data without arm and leg data. We proposed this technique, which consists of ellipse detection, Z-cross section cloud point rearranging and ellipse segmentation by circumference techniques, in [20]. First, by projecting 3D body coordinate that have euclidean distance less than condition on vector, it can detect a number of ellipses as shown in Fig. 3.5 (b). Second, when getting a number of ellipses, we rearranging cloud points in Z-cross section because coordinate order of 3D body data does not sort orderly. If we do not rearrange the cloud points and find ellipses more than one, we cannot separate ellipses to individual. Finally, in order to segment arm and leg data out from the 3D body data, they are segmented ellipse size by circumference techniques because we store every ellipse size in 3D body data to calculate mean value. Moreover, it is used to be condition for segmenting torso data. The condition is that if their circumference more than the mean value, they will define torso data as shown in Fig. 3.5 (c) (blue points). On the another hand, unless circumference less than the mean value, they will define arm and leg data as shown in Fig. 3.5 (c) (green points). The result of body segmentation is shown in Fig. 3.5 (d) and examples of results are shown in Table 3.2.

(a)	(b)
(c)	(d)
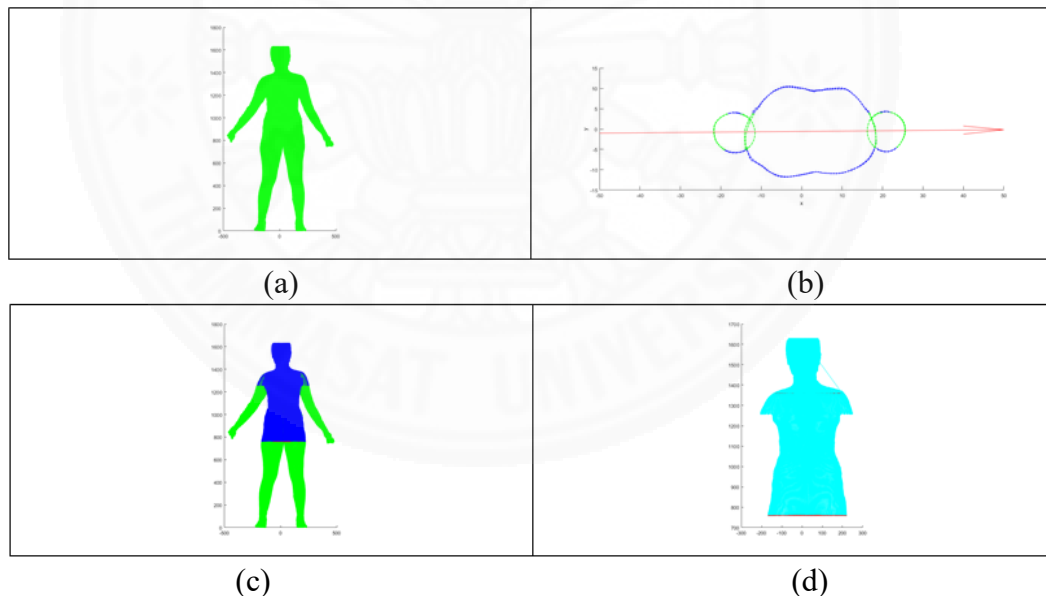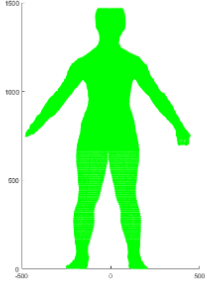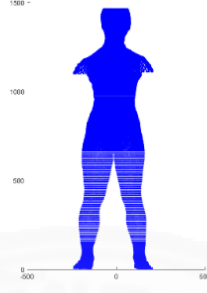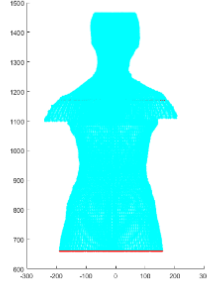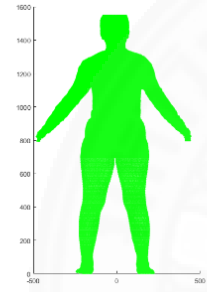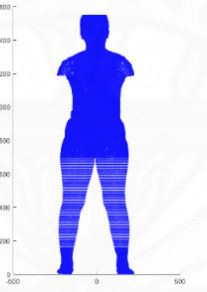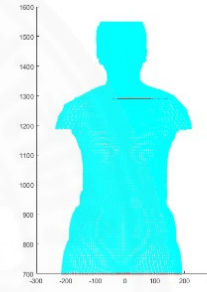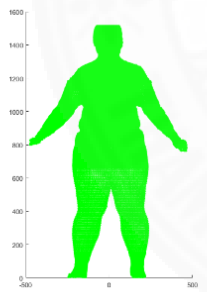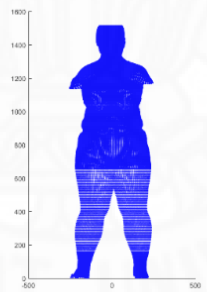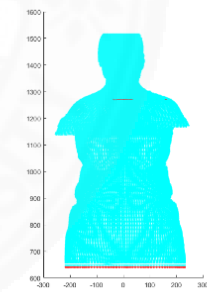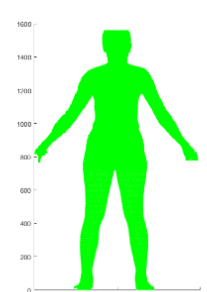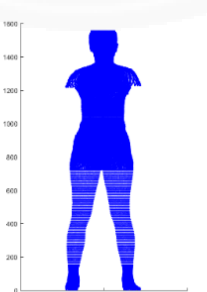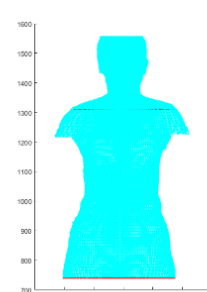
Fig. 3.5 Body segmentation method start from (a) input data, (b) Z-cross section projecting on vector, (c) body segmenting and (d) result of body segmentation.

Table 3.2 Examples of body segmentation results

Input data	Body segmentation methodology	Result of body segmentation

3.1.3 body landmark detection and measurement

Body landmark detection and measurement method can detect 5 human body landmarks that consist of bust, small of back waist, maximum waist, minimum waist and hip. We proposed in [11]. The purpose of this method is to detect and measure the circumference of human body landmark in order to prepare these data for the human body shape clustering part.

3.1.3.1 Bust detection methodology

This methodology can be divided into 5 steps described as follows:

1. By projecting torso data into sagittal plane, we can find front edge of the torso data from maximum value of anterior-posterior value called "y value" in vertical axis levels as shown in Fig. 3.6 (a).
2. When we calculate slope between 2 points from top to bottom, the slopes can be divided into 2 groups which are positive and negative slope as shown in Fig. 3.6 (b).
3. If slopes change from positive to negative at least 4 point, their heights and a constant that is calculated by Eq. (3.6) will be stored as shown in Fig. 3.6 (c).

$$constant = 20 * \frac{(Mean\ Z + range\ Z)}{100}$$

(3.6)

Where *MeanZ* is average height in vertical axis of torso data.

rangeZ is maximum – minimum value in vertical axis of torso data.

4. Bust region is defined by finding farthest point from central axis of the torso data and expanding from farthest point in range of [-50, 50]. Moreover, bust circumference is defined by maximum circumference in the bust region as shown in Fig. 3.6 (d). Examples of this method are shown in Table 3.3.

17

(a)   (b)

(c)   (d)
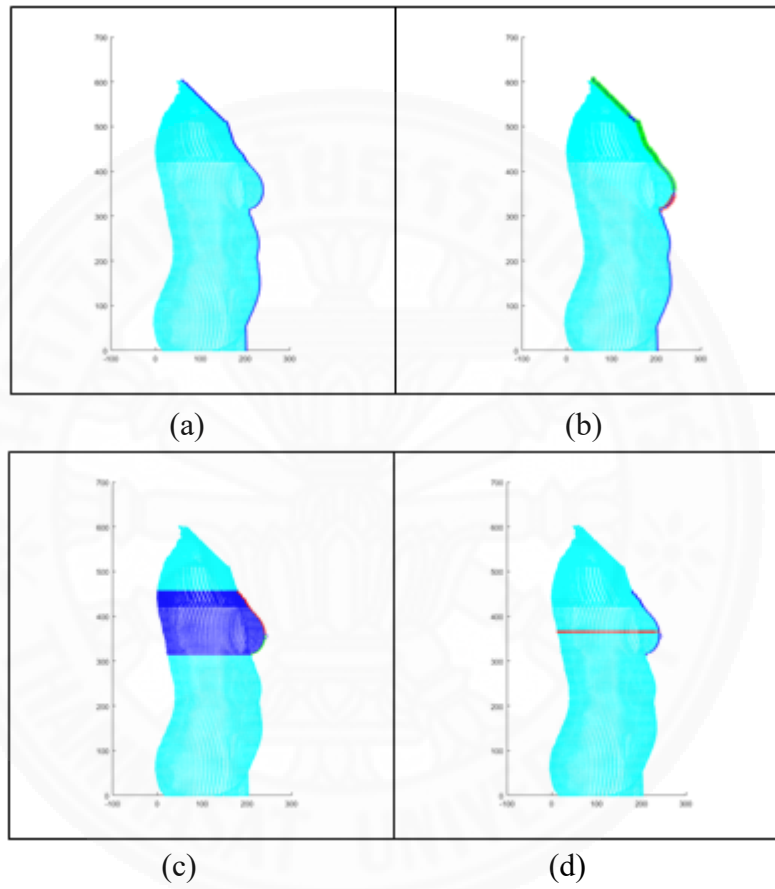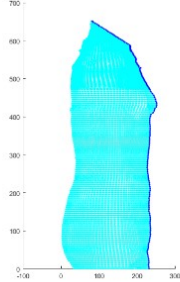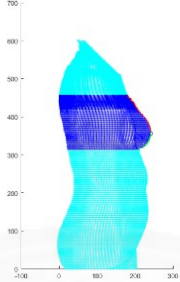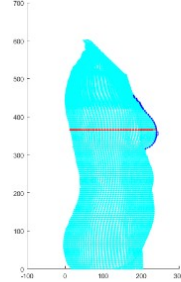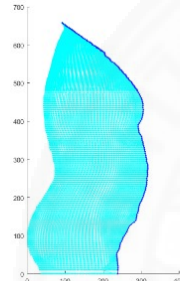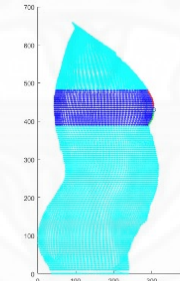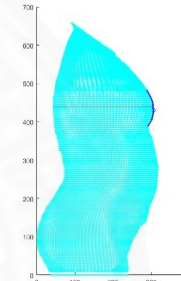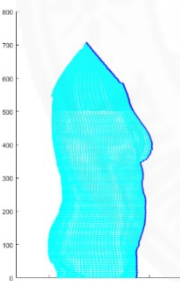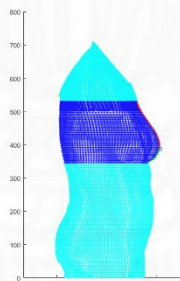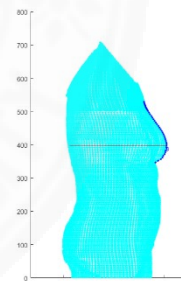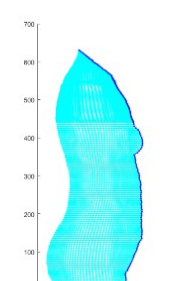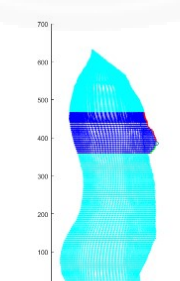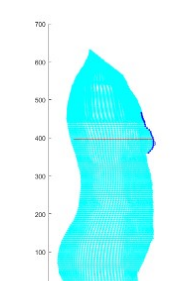
Fig. 3.6 Bust detection method start from (a) Front edge detection, (b) slope pattern detection, (c) bust region defining and (d) bust circumference detection.

Table 3.3 Examples of bust detection methodology

Input data	Bust detection methodology	Result of bust detection

19

3.1.3.2 Hip detection methodology

This methodology can be divided into 5 steps that is similar to bust detection methodology but differ some steps. It is created to detect hip in 3D body data, which is a texture coordinate without vertex color. This methodology is described as follows:

1. By projecting torso data into sagittal plane, we can find back edge of the torso data from minimum value of anterior-posterior value called "y value" in vertical axis levels as shown in Fig. 3.7 (a).

2. When we calculate slope between 2 points from bottom to top, the slopes can be divided into 2 groups which are positive and negative slope as shown in Fig. 3.7 (b).

3. If slopes change from negative to positive at least 4 point, their heights and a constant that is calculated by Eq. (3.6) will be stored as shown in Fig. 3.7 (c).

4. Hip region is defined by finding farthest point from central axis of the torso data and expanding from farthest point in range of [-80, 80]. Moreover, hip circumference is defined by maximum circumference in the hip region as shown in Fig. 3.7 (d). Examples of this method are shown in Table 3.4.

(a)	(b)
(c)	(d)
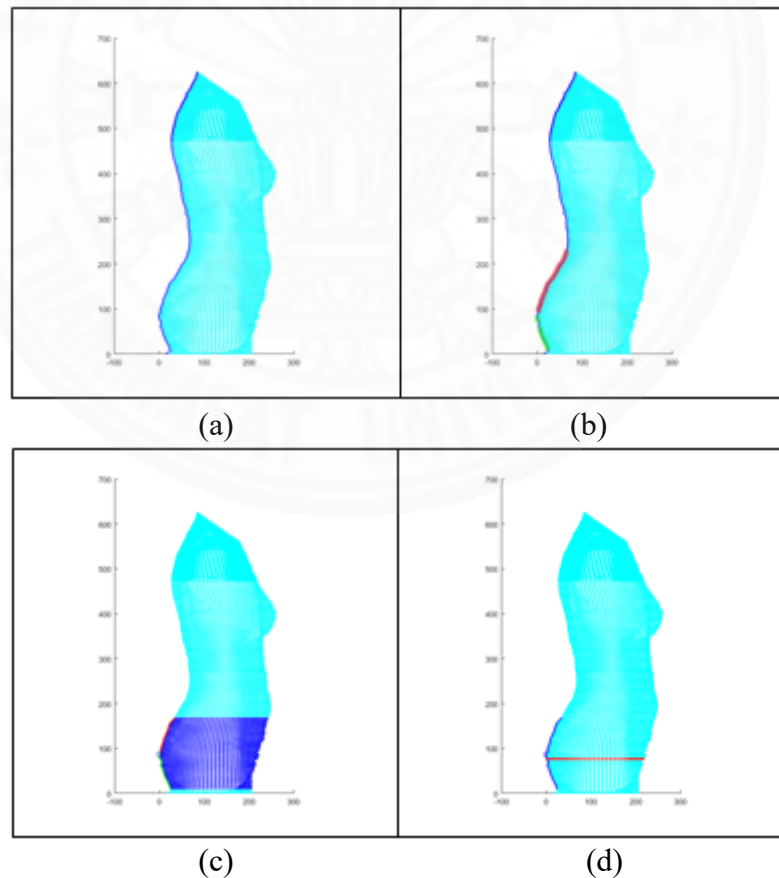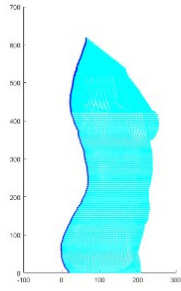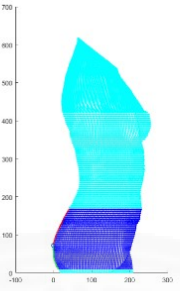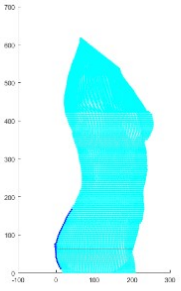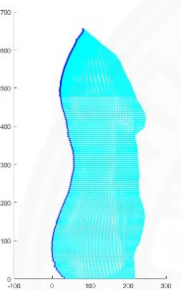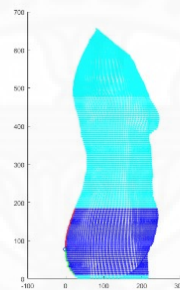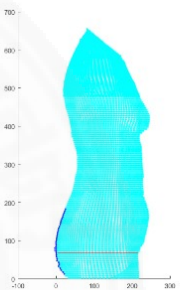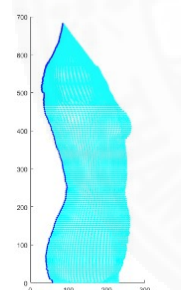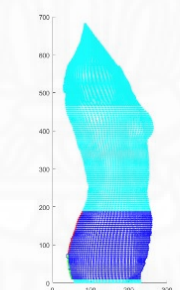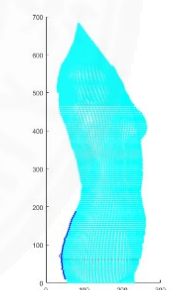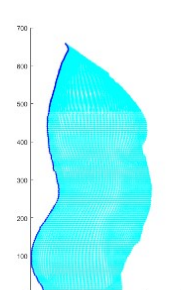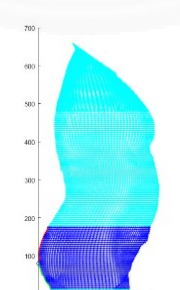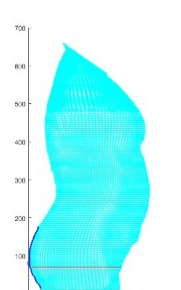
Fig. 3.7 Hip detection method start from (a) Back edge detection, (b) slope pattern detection, (c) hip region defining and (d) hip circumference detection.

Table 3.4 Examples of hip detection methodology

Input data	Hip detection methodology	Result of hip detection

3.1.3.3 Waists detection methodology

This methodology is created to detect waists that are small of back, maximum waist and minimum waist in 3D body data. It can be divided into 5 steps that is similar to bust detection methodology but differ some steps. This methodology is described as follows:

1. By projecting torso data into sagittal plane, we can find both front and back edge of the torso data from bust and hip detection methodology shown in Fig. 3.8 (a).

2. When we calculate slope between 2 points from bottom to top, the slopes can be divided into 2 groups which are positive and negative slope.

3. If slopes change from negative to positive at least 4 point, this region is defined to small of back waist as shown in Fig. 3.8 (a).

4. Maximum and minimum waist region is defined by finding small of back waist point from central axis of the torso data and expanding from small of back waist point in range of [-50, 50] as shown in Fig. 3.8 (b). Moreover, maximum waist circumference is defined by maximum circumference in this region. On the another hand, maximum waist circumference is defined by maximum circumference in this region as shown in Fig. 3.8 (c) and (d). Examples of this method are shown in Table 3.5.

(a)   (b)

(c)   (d)
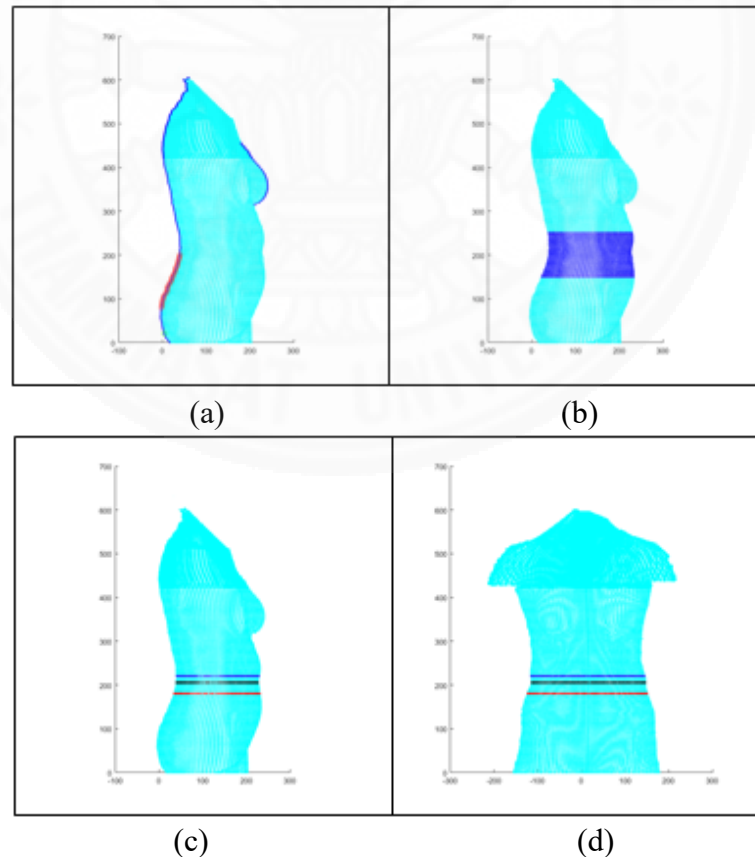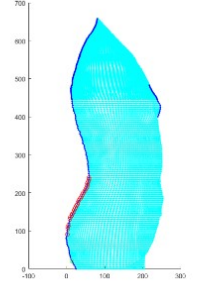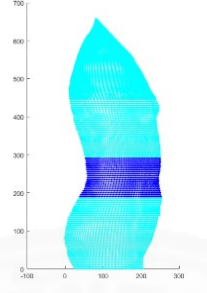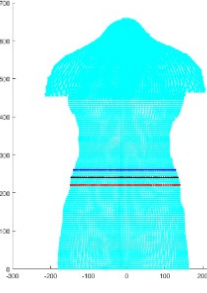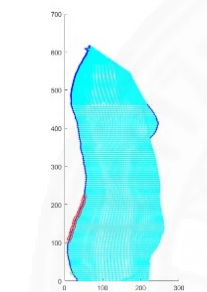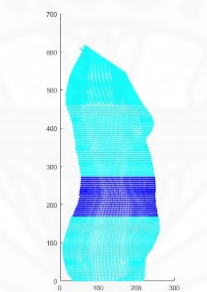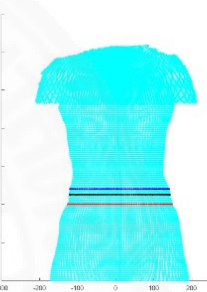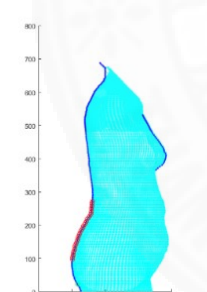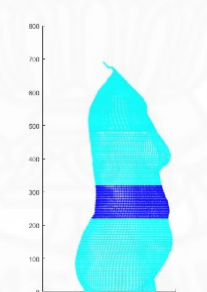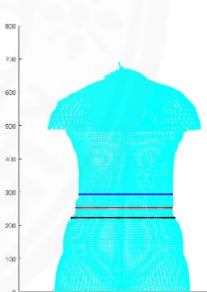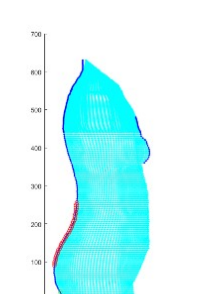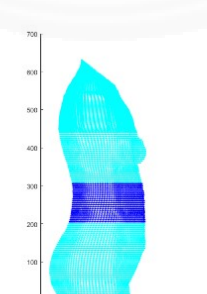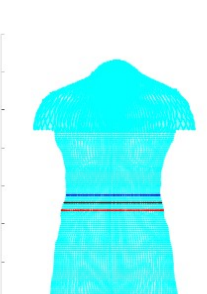
Fig. 3.8 Waists detection method start from (a) Front and back edge from previous methodology, (b) waist region defining, (c) waists circumference detection in side view and (d) waists circumference detection in front view.

22

Table 3.5 Examples of waists detection methodology

Input data	waist detection methodology	Result of waists detection

3.2 Experimental results and discussion

In this section, we purpose experimental results of human body analysis algorithm. These experimental results are divided into 3 parts that consist of experimental result of plane adjustment, body segmentation as well as body landmark detection and measurement. First, section 3.2.1 describes accuracy of plane adjustment algorithm. Second, accuracy of the body segmentation algorithm is described in section 3.2.2. Finally, section 3.2.3 explains the performance of body landmark detection and measurement. Body landmarks consist of bust, small of back waist, maximum waist, minimum waist and hip. All of those are experiment result of data preparation for using in human body shape clustering part, which is described in Chapter 4.

3.2.1 Accuracy of plane adjustment algorithm

We evaluate an accuracy of plane adjustment algorithm. A definition of correct result is that 3D body data have same face direction, standing position and same height. On the another hand, if the 3D body data have some different condition, it will be failure result. By evaluating the accuracy of the experiment result calculates into percentage from Eq. (3.7) and (3.8). Table 3.6 summaries accuracy of experiment result of this plane adjustment algorithm.

$$Number\ of\ success = Number\ of\ 3D\ body\ data\ \text{-}\ Number\ of\ failure$$

(3.7)

$$Accuracy\ of\ this\ algorithm = Number\ of\ success\ /\ Number\ of\ 3D\ body\ data\ \text{x}\ 100\%$$

(3.8)

Table 3.6 Accuracy of plane adjustment algorithm

Methodology	Number of failure	Number of success	Accuracy (%)
plane adjustment (90)	0	90	100.00

3.2.2 Accuracy of body segmentation algorithm

In this section, accuracy of the body segmentation algorithm is evaluated by using the ground truth data in extracted data from software included in [TC]²'s scanner. The ground truth called "wrl file" is manually extracted by the [TC]²'s software. Experiment result of body segmentation is compared by the ground truth in order to calculate its accuracy. By evaluating the accuracy calculates into percentage from Eq. (3.7) and (3.8). Table 3.7 summaries accuracy of experiment result of body segmentation algorithm.

24

Table 3.7 Accuracy of body segmentation algorithm

Methodology	Number of failure	Number of success	Accuracy (%)
body segmentation (90)	0	90	100.00

3.2.3 Accuracy of body landmark detection and measurement algorithm

Accuracy evaluation of this methodology is that its experiment result compare with extracted data from [TC][2]'s software included in its 3D scanner. The extracted data called "ord file", which is manually extracted. This accuracy calculation is used to evaluate the experiment result of bust, small of back waist and hip without maximum and minimum waist because there is no both of them. The comparison consists of the circumference and height of the body landmarks. By evaluating the accuracy of the experimental result calculates into percentage from Eq. (3.7) and (3.8). Moreover, accuracy of the experiment result of this algorithm is summarized by referencing the location of the body landmarks as shown in Table 3.8 and by referencing circumference of the body landmarks as shown in Table 3.9.

Table. 3.8 Accuracy of body landmark detection and measurement algorithm by referencing location

Methodology	Number of failure	Number of success	Accuracy (%)
Bust detection(90)	0	90	100.00
Waist detection	2	88	97.78
Hip detection	0	90	100.00

Table. 3.9 Accuracy of body landmark detection and measurement algorithm by referencing circumference

Methodology	Number of failure	Number of success	Accuracy (%)
Bust detection(90)	0	90	100.00
Waist detection	4	86	96.67
Hip detection	1	89	98.89

In sum, according Table 3.8, it shows that the data acquisition methodology can extract important data from 3D body data without depending the software included with 3D scanner. Accuracy is 100.00, 97.78 and 100.00 percent when compared with location in [TC][2]'s extracted data. Moreover, accuracy is 100.00, 96.67 and 98.89 percent when comparing with a circumference in [TC][2]'s extracted data. Therefore, the data acquisition methodology has enough efficiency to using for human body shape clustering part in Chapter 4.

Chapter 4

Human body shape clustering methodology and experimental result

This chapter describes human body shape clustering methodology, which is the second part of this thesis. There are human body shape clustering methods referred to in Chapter 2. Most of they need to fix a number of final group or are appropriate with data that has a few groups. In this thesis, we propose a dynamic method that does not need to fix a number of final groups and is flexible. This method is an algorithm based on Particle Swarm Optimization (PSO), which is designed in order to cluster 3D human body shape. The detail of methodology and experimental results are described in this chapter.

4.1 Methodology

Human body shape clustering methodology can be divided into 3 parts that consist of fitness function creation, preprocessing of PSO and human body shape clustering based on PSO as shown in Fig. 4.1. The purpose of this methodology is a fitness function creation that is used to optimize 3D human body shape clustering, the best environment of PSO searching for the best performance of experimental result and human body shape clustering based on PSO. Section 4.1.1 describes the fitness function in this thesis. Moreover, preprocessing of PSO method looks for the best suitable parameters that affect PSO's performance and it is explained in section 4.1.2. Finally, in section 4.1.3, we propose a 3D human body shape clustering based on PSO. The details of each step are described as follows:
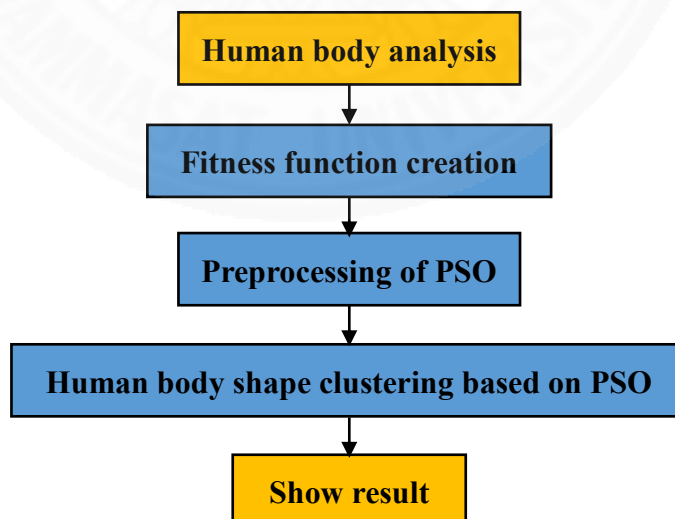
Fig. 4.1 Human body shape clustering methodology flowchart.

4.1.1 Fitness function creation

A fitness function is a particular type of objective function. The fitness function is an equation that is used to minimize optimal solution of problem in programming techniques. It can be the result of an attempt to express a goal in mathematical terms for using in optimization studies. In this thesis, the fitness function is used for minimizing optimal solution of 3D human body shape clustering. We create it from the combination between volumetric and anthropological difference. First, volumetric difference is the volume that overlaps between two different data. It is volume in part that is not superimposed together. This volume is calculated by Eq. (4.1) and shown as Fig. 4.2. Second, anthropological difference is the dissimilarity of body measurement rations that is measured by Eq. (4.2). Finally, both of the volumetric and anthropological difference are combined by Eq. (4.3), which is the fitness function in order to calculate similarity between two 3D data. The similarity value is a score that measures the difference between them and is used for similarity indicator in this thesis. Furthermore, a system fitness function described by Eq. (4.4) is used to measure system similarity value.
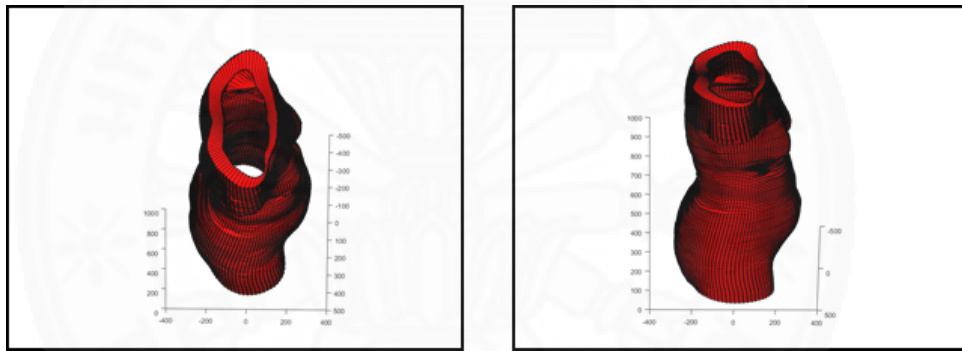
Fig. 4.2 The volumetric overlap between two 3D data.

First, this Eq. 4.1 can calculate the volumetric difference between two 3D body data. By measuring volume that is not superimposed together of volume divided into three part, it express a dissimilarity more clearly than the volume that does not be separated. The volumetric difference is presented in Fig. 4.3 that is three part of divided volume. A reason that we separate it in to three part is an improvement of volumetric difference comparing between two 3D body data. Because in first experiment, we did not divide it, it causes conflict in some data. The advantage of separating volume is that it is able to indicate clearly the dissimilarity in each part of volumetric overlap. For example, it can present the dissimilarity although both two 3D body data have the same bust and hip but have different waist. This volume is calculated by Eq. (4.1) and shown as Fig. 4.3.

$$V(i,j) = \sqrt{\frac{1}{z}\sum_{n=1}^{z}\left(\sum_{f=h_{z-1}}^{h_z} A(B_i, B_j)\right)}$$

(4.1)

Ref. code: 25595822040050POR

Where $V(i,j)$ is volumetric overlap between 3D body data B_i and B_j, i is the active user, j is a user provided by the profile selection process, where $j \neq i$, Z have three part where Z is number of Z-cross section, h_z is height of 3D body in each Z-cross section, $A(B_i, B_j)$ is area overlap between 3D body data B_i and B_j on Z-cross section between zeros to height, B_i and B_j is cloud point of 3D body data vector.
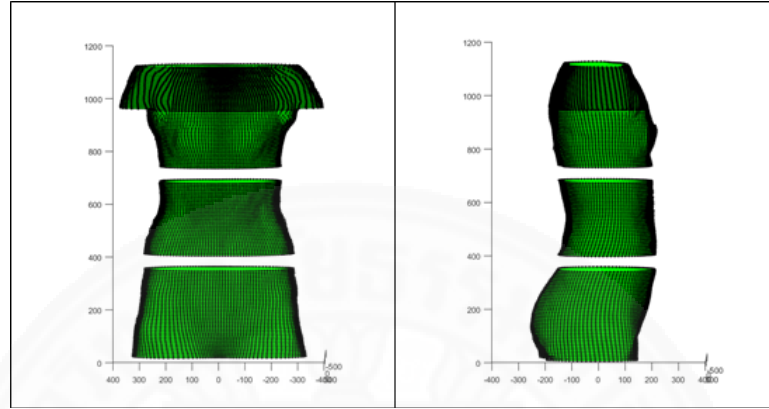
Fig. 4.3 The three body regions of volumetric overlap between two 3D data in our progress [11].

Second, the Eq. 4.2 can measure the anthropological difference. By calculating based on Euclidean distance, it is able to measure the dissimilarity of each feature. In this thesis, we use feature that is the ratios between body landmarks in order to evaluate the anthropological difference. They consist of the ratios between bust, maximum waist, minimum waist, small of back waist and hip that is mentioned in Chapter 3 and is shown in Fig. 4.4. The bust region is a blue line, the minimum waist region is a black line, the maximum waist region is a yellow line, small of back waist region is a red line and the hip region is a green line. All of feature are follows:
1. The ratio between bust and hip.
2. The ratio between bust and minimum waist.
3. The ratio between bust and maximum waist.
4. The ratio between bust and small of back waist.
5. The ratio between hip and minimum waist.
6. The ratio between hip and maximum waist.
7. The ratio between hip and small of back waist.
8. The ratio between minimum waist and maximum waist.
9. The ratio between minimum waist and small of back waist.
10. The ratio between maximum waist and small of back waist.

$$euclidean(i,j) = \sqrt{\frac{1}{z}\sum_{f=1}^{z} diff_{k,f(i,j)^2}}$$

(4.2)

28

Where $euclidean(i,j)$ is Euclidean distance of body measurement ratios, i is the active user, j is a user provided by the profile selection process, where $j \neq i$, k is the number of features. $diff_{k,f(i,j)}$ is the difference in profile value for feature f between users i and j on feature k.
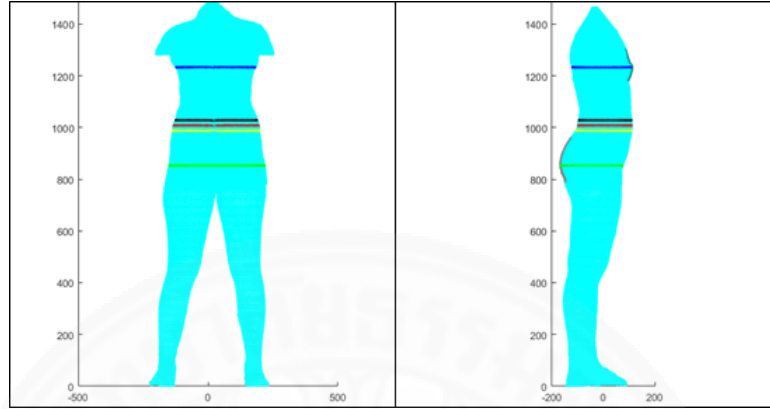
Fig. 4.4 The regions for calculating the anthropological difference in our progress [11].

Moreover, this Eq. 4.3 is an equation that is used to calculate the similarity between two 3D body data in this thesis. By combining between the volumetric and anthropological difference, it is able to measure clearly the difference. A reason that we have to combine both difference into fitness function because the experimental result of 1st version of our PSO algorithm presented in our progress [20]. It shows that the only volumetric difference could not efficiently compare the similarity or it has limitation of volumetric fitness function. Therefore, we experiment 2nd version of our PSO algorithm with adding an anthropological difference into fitness function. Its result is satisfying and it can solve the limitation problem of volumetric fitness function in 1st version. Furthermore, the similarity value is a score that measures the difference between them and is used for similarity indicator.

$$Fitness(i,j) = w_e\ euclidean(i,j) + w_v\ V(i,j)$$

(4.3)

Where $Fitness(i,j)$ is fitness score between user i and j, w_e is the weight for feature $euclidean(i,j)$ and w_v is the weight for feature V_{ij}, where $w_e + w_v = 1$.

Finally, the similarity value of system that is used to measure the difference between member in each group is calculated by Eq. 4.4. It is able to indicate the minimum dissimilarity that our PSO algorithm can do. All of the equations are a fitness functions that are used to solve the problem of the 3D human body shape clustering based on PSO algorithm. They show the performance that they are able to divide 3D body data into groups without the need of model, training and a number of the final group as mentioned at the at the experimental result of human body shape clustering based on PSO in section 4.2.2.

29

$$Fitness\ System\ = \sum_{i=1}^{n} \sum_{j=1}^{m} Fitness(i,j)$$

<div align="right">(4.4)</div>

Where $Fitness\ System$ is System fitness score, i is the active user, j is a user provided by the profile selection process, where $j \neq i$, m is number of user i's neighborhoods, n is number of user in swarming space.

4.1.2 Preprocessing of PSO

Preprocessing of PSO is a methodology that looks for the best parameters of PSO for the best performance. This methodology is essential importance for our thesis because it does not only search for suitable environment of PSO but also reduce working time. Without it, we will spend much time for the experimental result in heavy load conditions. Unless we use it before PSO test, it will be better than previous one. This methodology used test data that are divided into 3 groups and balanced a number of their members. The test data consists of 10 and 90 users. Moreover, the parameters of this method consist of swarming space size, maximum radius of neighborhood, maximum of velocity and repulsive factor. Finally, we describe other parameters associated with the PSO algorithm and Swarm Diagrams that is used in this thesis in section 4.1.2.5 and 4.1.2.6.

4.1.2.1 Swarming space size

Swarming space size is defined as space within that particle or user move. The space is used as area for moving of particles that have appropriate scales for population in the space. We attempt to find the size of the swarming space in order to get the best experimental result. We divide experiments into 4 cases, such as 1500, 3000, 13500 and 27000 units per each dimension, as shown in Table. 4.1, so that we look for the suitable space size for different populations.

Table 4.1 Swarming space sizes list

Size 1 (the original size for 10 users)	1500
Size 2 (twice the size Size1)	3000
Size 3 (the original size for 90 users, as size 1 was shown to work well for 10 users which equates to 150 units per user, applying this ratio for 90 users gives 13500)	13500
Size 4 (twice the size of Size3)	27000

4.1.2.2 Maximum radius of neighborhood

The maximum radius of neighborhood is the maximum range of seeing ability in each particle. In order to be fair, a constraint applied to this variable and the value does not have to exceed the swarming space size. This radius has a considerable relation with a meeting rate in our PSO algorithm. For example, if this range is too

<div align="center">30</div>

long, the particle will meet too many neighborhoods and it causes too much load of our PSO algorithm. On the another hand, if this range is too short, it causes resulting clusters tried to swarm together in the center. Therefore, the most suitable range searching is the best way in order to improve the performance of our PSO algorithm. This experiment is divided into 4 parts that consist of 50, 100, 150 and 200 unit as shown in Table 4.2.

Table 4.2 Maximum radius of neighborhood list

Range 1 (half the original range)	50
Range 2 (the original range)	100
Range 3 (One and a half times the original range)	150
Range 3 (Twice times the original range)	200

4.1.2.3 Maximum of velocity

Maximum of velocity is the particle's fastest speed that have value in range [-vmax, vmax]. Due to its variation, the maximum of velocity affects to the different neighborhood meeting. For example, if the maximum of velocity is too low, particle will have a low chance of neighborhood meeting. Unless the maximum of velocity is too high, particle will lose his neighborhood. Therefore, a suitable maximum of velocity searching is essential for this thesis because it can reduce a number of iteration in each run. This experiment is divided into 4 cases that are 50, 100, 150 and 200 units per move as shown in Table 4.3.

Table 4.3 Maximum of velocity list

Velocity 1 (half the original velocity)	50
Velocity 2 (the original velocity)	100
Velocity 3 (One and a half times the original velocity)	150
Velocity 3 (Twice times the original velocity)	200

4.1.2.4 repulsive factors

Repulsive factors are proposed in [28]. It is pushing force in order to avoid outsider or unwelcome users from entering the neighborhood. It has a greatly relation with a grouping performance in this thesis. This experiment have 3 cases, such as zero which is no repulsive force, one which causes the active user to move away form the outsider and two which has twice the effect as previous value. All of them is shown in Table 4.4.

31

Table 4.4 Repulsive factors list

Factor 1 (no repulsive force)	0
Factor 2 (causes the active user to move in the direction opposite to the outsider)	1
Factor 3 (has twice the effect as factor 2)	2

4.1.2.5 Other parameters associated with the PSO algorithm

Other parameters associated with the PSO algorithm are described as follows. *lbest* or *gbest*, which this thesis use *lbest* and call "*nbest*", is neighborhood position and have the minimum fitness score. The *pbest* is the central position of friend. Friend is user that active user met and his fitness score less than threshold. Maximum number of friend is a number of friends that particle can have. Threshold in this experiment is set to 0.5. Test data is divided into 3 groups. Members in the same group are provided a fitness score in range [0, 0.5]. On the other hand, the fitness score between different group is given in range [0.6, 1]. We test them in all possible conditions that is 192 cases and they are governed by from the 1st to 4th rules (Eq. (2.1), (2.2), (2.3), (2.4)).

$$v_i = wv_i + c_1r_1(x_{pbest,i} - x_i) + c_2r_2(x_{gbest,i} - x_i) \quad \text{Rule 1}$$
$$v_i = v_i + f_3c_3r_3(x_{avoid,i} - x_i) \quad \text{Rule 2}$$
$$if(|v_i| > v_{max}) \quad v_i = (v_{max}/|v_i|)v_i \quad \text{Rule 3}$$
$$x_i = x_i + v_i \quad \text{Rule 4}$$

Where x_i is the current position of particle i

x_{pbest} is the best friend position attained by particle i

x_{gbest} is the swarm's global best position

x_{avoid} is the all outsider position attained by particle i

v_i is the velocity of particle i

w is a random inertia weight between 0.5 and 1 [26]

c_1, c_2 and c_3 are spring constants whose values are set to 1.494 [26]

r_1, r_2 and r_3 are random numbers between 0 and 1 [27]

f_3 is the repulsive factor

The preprocessing PSO algorithm is modified from the modified PSO in [28]. We change the algorithm in part of the evaluation of fitness function, a number of maximum friends and neighborhoods in order to search the best environment of PSO.

4.1.2.6 Swarm Diagrams

Swarm Diagrams are tools that use for analyzing PSO's behavior in order to reduce time of analysis by hand. They are created by Supiya Ujjin in [28] and They consist of average *pbest* movement, Swarm Activity, System Fitness Score, *pbest* movements display and swarm path display. We use them as follows:

1. The average *pbest* movement is used to track the change of average *pbest* movement in the PSO system. It can indicate a convergence of average *pbest* speed.
2. The swarm Activity is used for following the trend of particles' speed in the PSO system. It can display a convergence of particles' speed.
3. The system Fitness Score is indicator that can express the minimum fitness value presenting the performance of our PSO algorithm.
4. *The pbest* movements display is use to assist us in order to see moving of the particles' *pbest* position in the space and verify correctness easier.
5. The swarm path display helps us clearly seeing moving of particle in the space and easily tracking individual's behavior.

4.1.3 Human body shape clustering based on PSO

A 3D body shape clustering algorithm is mentioned in Chapter 2. There are diverse researches that relate it, such as training, model recognizing or fixing a number of the final group. Although, there are several research, we want to avoid all of them. However, in this thesis, we proposed the idea of the 3D body shape clustering algorithm based on PSO without the need to use model and fix a number of the final group. Moreover, we proposed progresses of this thesis in [11, 20] and they are clustering algorithm based on PSO. Particle swarm optimization (PSO) is a population based stochastic optimization technique developed by Eberhart R. C. and Kennedy J. [21]. It exhibits self-organization and searches the solution space for optima through iterative procedures. Moreover, Supiya Ujjin proposed a modify PSO [28] that adds another variable called "outsider" which is the position that needs to avoid by using a repelling force. It is this modified PSO algorithm that is employed in this work.

4.1.3.1 New attributes of clustering algorithm based on PSO

We contribute new attributes of our clustering based on PSO algorithm. They consist of the fitness function for solving a 3D human body shape clustering problem, the best environment of PSO for solving our problem, update of assembly point by using the point at previous round, no need to fix a number of maximum friend and a number of maximum round of run that has converged. We describe as follows:

1. The fitness function is the objective function that is used to solve a 3D human body shape clustering problem. It has to be appropriate for our problem and It is mentioned in section 4.1.1.

2. The best environment of PSO is the parameters that our PSO algorithm need to have in order to solve our problem best. It is mentioned in section 4.1.2.
3. Update of assembly point by using the point at previous round is a method to use the benefit of previous meeting point for increasing a chance of particle encounter.
4. A maximum number of friend do not need to fix for giving more chance in order to keep tracking particles' friend or similar user.
5. A number of maximum round of run having converged is added to our PSO algorithm. Due to its benefit, we use it to increase meeting rate of particles. It is set to 10 round. In each round, particles begin with random position and velocity before their activity will have converged or speed will have 0 value.

All of they are added in our human body shape clustering based on PSO algorithm so that this algorithm has perfectly performance for solving the problem.

4.1.3.2 Progress of clustering algorithm based on PSO

We attempt to find the best experimental result of the human body shape clustering based on PSO algorithm. By using different fitness function, there are 4 versions that describe as follows:

1. First version used only volumetric fitness function and assembly point update by centroid of particles' current point. It was proposed in [20] or our first paper, but the proposed fitness function was too rigid that resulting clusters tried to swarm together in the center.
2. Second version was added anthropological difference of 3D body data to fitness function called "Euclidean distance fitness function" in this thesis. In this version, we combined the fitness function between volumetric and Euclidean distance fitness function together so that we want to improve performance of our fitness function, but it could not solve problem of previous version.
3. Third version divided volumetric fitness function into 3 parts by height of 3D body data in order to increase clarity of volumetric difference. This version was able to solve problem of previous version. It was proposed in [11] or second paper.
4. Fourth version change an update method of assembly point from centroid of particles' current point to assembly point at previous round in order to increase meeting rate of particles.

In this thesis, we describe 4th version of the human body shape clustering that is the latest and best version. By finding the relationship between weight of fitness function and threshold, they will be the best condition for solving body shape clustering problem. The weight of fitness function is a ratio of volumetric overlap to Euclidean distance fitness function.

34

4.1.3.3 The Clustering based on PSO Algorithm

The important factors of PSO algorithm consist of swarming Space, users as particles, neighborhood of friends, neighborhood selection, all of which are presented by Supiya Ujjin in [28]. We describe as follow:

1. The swarming space in this thesis is an unbounded space in N dimensions so that it can improve particles' vision ability. It causes a meeting rate of particle increasing.
2. The users as particles is a kind of data vision in our PSO algorithm. It see the 3D body data that has more details as one particle in order to work easily.
3. The neighborhood of friends is a type of neighborhood in swarming space. They consist of friend and outsider. A friend is particle that has a similarity less than or equal to threshold. On the another hand, an outsider is particle that has a similarity more than threshold.
4. The neighborhood selection is an updating process of a position and velocity. This processing consists of neighborhood checking, similarities evaluation, neighborhood best updating, best friend updating and outsiders updating, some of which are adopted and modified for using in this thesis.

The most essential part is the clustering algorithm based on PSO that is modified from Supiya Ujjin's algorithm. Besides our new attributes, the modified part is describe as follows:

1. To count converged swarm activity instead of fixing a number of maximum iteration.
2. To compare body size before evaluate fitness function in order to decrease load in our PSO algorithm.
3. To change the friend lists updating from the best neighborhood adding to similarity checking of neighborhood. If his neighborhood has a similarity less than threshold, it will be added into his friend list.
4. To add the assembly point of each group at previous round of run in order to improve meeting rat of particle.

All of they are changed parts for according the new attributes that we added to our PSO algorithm. The clustering based on PSO algorithm is shown in figure 4.5 and our modified parts are highlighted.

```
1    The profile creation processing
2    LOOP 1
3        LOOP 3
4            LOOP 4 for each active user, A, in current Profile Selection set
5                The neighborhood checking processing
6                if A's neighborhood is not empty
7                    LOOP 5 for each user j in A's neighborhood
8                        if A's body size equals to j's body size
9                            Compute fitness score between A and j, Fitness(A, j)
10                           if fitness score more than threshold
11                               Remove j from neighborhood
12                               Add j to A's outsider list
13                           else
14                               if A's best friend list is empty
15                                   Add j to best friend list
16                               else
17                                   if there is not j in A's best friend list
18                                       Add j to best friend list
19                       else
20                           Remove j from neighborhood
21                           Add j to A's outsider list
22                   END LOOP 5
23                   The neighborhood best updating processing
24                   if A's best friend list is empty
25                       Set A's Xpbest in Rule 1 to be nbest's current position
26                   else
27                       if round is first round
28                           Update A's Xpbest in Rule 1 to be the current central position of A's all best friends
29                       else
30                           Update A's Xpbest in Rule 1 to be nbest's current position
31                   if A's outsider list is not empty
32                       Set A's Xavoid in Rule 2 to be the central position of all users in the list
33                   else
34                       Set a flag that A's Xavoid is not used in this iteration
35               else (A's neighborhood is empty)
36                   if A's best friend list is empty
37                       Set A's Xpbest in Rule 1 to be the central position of all users in the system
38                   else
39                       if round is first round
40                           Update A's Xpbest in Rule 1 to be the current central position of A's all best friends
41                       else
42                           Update A's Xpbest in Rule 1 to be the assembly point of each group in (N-1) round
43                   Set a flag that A's Xnbest is not used in this iteration
44               The position and velocity updating processing
45               Reset nbest and outsider list for A
46           END LOOP (END LOOP 4)
47           Increment the number of iterations by 1
48       UNTIL All of swarm activities have converged (END LOOP 3)
49   UNTIL maximum round is reached (END LOOP 2)
```

Fig 4.5 The algorithm describing the clustering based on PSO.

4.2 Experimental results and discussion

In this section, we propose experimental results of human body shape clustering algorithm. These results are divided 2 parts that consist of experimental results of preprocess of PSO and human body shape clustering based on PSO. First, the section 4.2.1 describes the experimental result of the preprocess of PSO. In addition, the another one is the experimental result of human body shape clustering based on PSO in section 4.2.2.

4.2.1 Experimental result of preprocess of PSO

Experimental results of the preprocess of PSO are divided into4 parts that are swarming space size, maximum radius of neighborhood, maximum of velocity and repulsive factor. They are examined by 2 systems that are 10 and 90 users and is described as follows.

4.2.1.1 Swarming space size

10 users examines for experiments of swarming space size 1 and 2. Moreover, 90 users examines for experiments of swarming space size 3 and 4. Fig. 4.6 presents a graph of the result that is the accuracy of swarming space size. In this figure, a red and gray bar are an experiment of the 10 users. We can see that size1 (1500) has accuracy higher than size2 (3000) because small scale of the space has a higher chance of meeting new user than big one. In addition, experiments of the 90 users are increased scale to 13500 because there is a problem of overcrowding from the too small space size. However, if we increase the space size, this problem will be solved. A yellow and blue bar is experiment of 90 users. We can see that size 3 (13500) has accuracy more than size 4 (27000) as same as the experiment of 10 users.
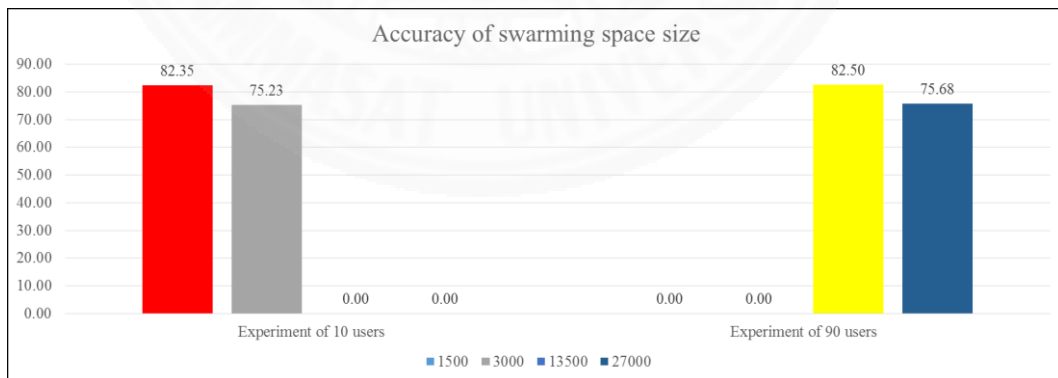
Fig. 4.6 Accuracy of swarming space size.

4.2.1.2 Maximum radius of neighborhood

Experiments of maximum radius of neighborhood show performance of seeing ability of particle. The maximum radius of the neighborhood that is range 4 giving highest accuracy of clustering as shown in Fig. 4.7. Furthermore, the experimental order presents that large range increase performance of PSO algorithm because there is a high chance of meeting other users. On the another hand, short range decreases

37

the performance. It is similar to swarm activity diagram that presents particle's movement in the space. If the range has small scale, particles will move in low level and constantly. Moreover, particles movement has converged faster than short range. However, if the range is too short, particles will move in high level or inconstantly as well as particle's movement has slowly converged because there is a low chance of meeting other particles. Swarm activity diagram is shown in Fig. 4.8 and 4.9.
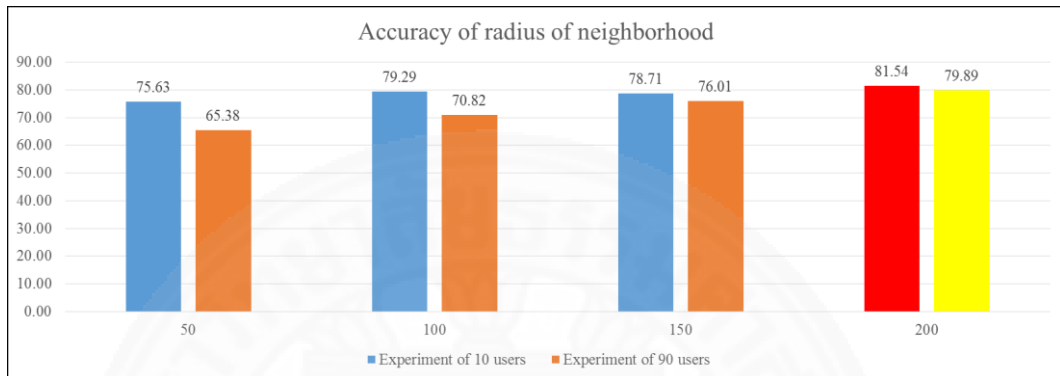
Fig. 4.7 Accuracy of maximum radius of neighborhood.
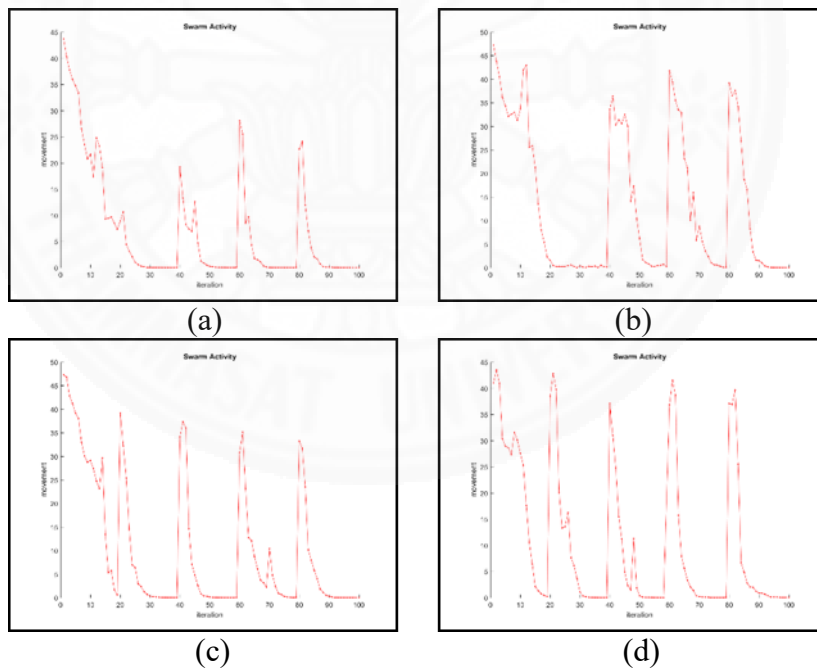
Fig. 4.8 Swarm activity of 10 users, (a) range 1, (b) range 2, (c) range 3 and (d) range 4.
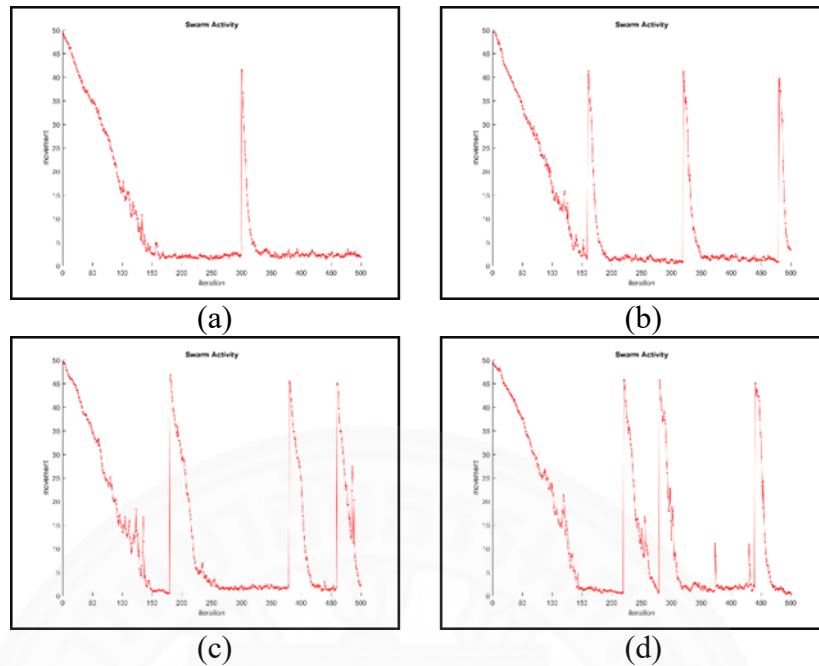
Fig. 4.9 Swarm activity of 90 users, (a) range 1, (b) range 2, (c) range 3 and (d) range 4.

4.2.1.3 Maximum of velocity

This section describes the experimental results of maximum of velocity as shown in Fig. 4.10. It is accuracy of maximum radius of neighborhood. In this figure, the best result is velocity 1 (50) and accuracy decreases when velocity increases. Because of the too high velocity, particles move more than they required and separate them into neighborhoods. According to Swarm activity diagram as shown in Fig. 4.11 and 4.12, when velocity increases, a number of swarm activity convergence decreases because too high velocity, such as velocity 3 (150) and velocity 4 (200), causes separated neighborhoods and looks for new ones again. Therefore, we should constrain maximum of velocity for tracking neighborhoods.
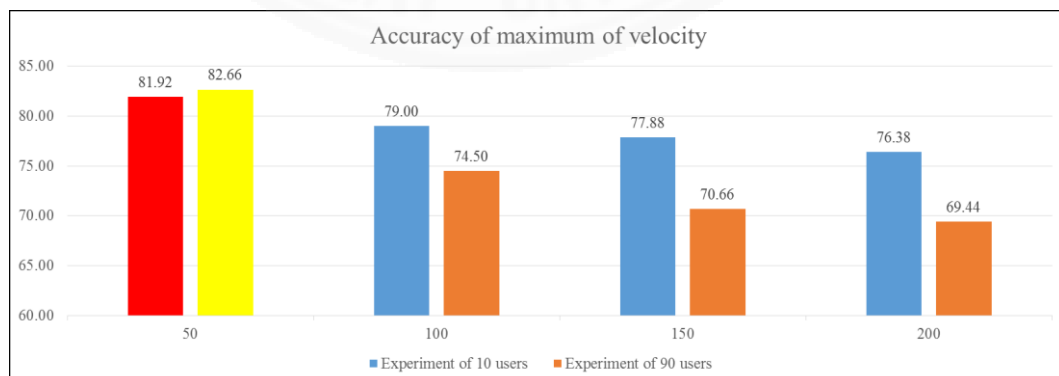
Fig. 4.10 Accuracy of maximum of velocity.

(a)

(b)

(c)

(d)
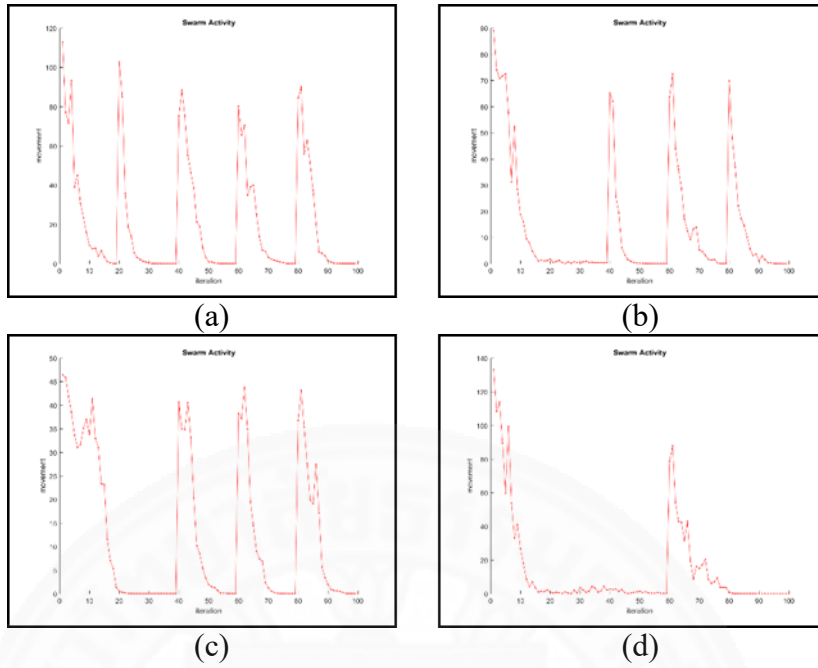
Fig. 4.11 Swarm activity of 10 users, (a) velocity 1, (b) velocity 2, (c) velocity 3 and (d) velocity 4.

(a)

(b)

(c)

(d)
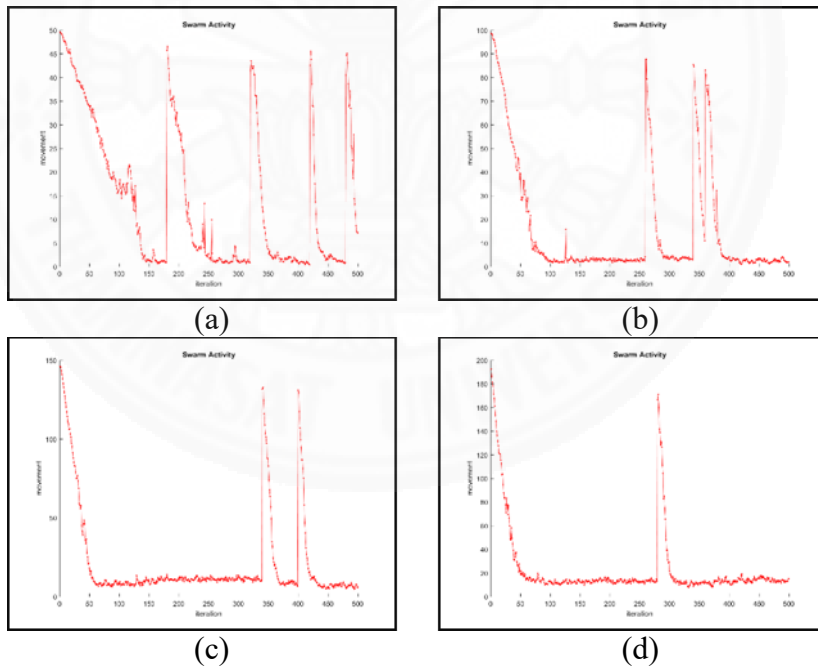
Fig. 4.12 Swarm activity of 90 users, (a) velocity 1, (b) velocity 2, (c) velocity 3 and (d) velocity 4.

40

4.2.1.4 Repulsive factor

Repulsive factor is used to separate outsider from the active user. The best experimental result of repulsive factor is factor 3 (repulsive factor equals to 2) as shown in Fig. 4.13. On account of particles' repulsion, members of different groups do not assemble into the same group as shown in Fig. 4.14 and 4.15. On the another hand, when there is on repulsive force, members of different groups mix into the same group. Due to no outsider avoidance, performance of clustering decreases. Swarm path displays show clearly in Fig. 4.15 (a) that if there is no repulsive force, assembled particles cannot be divided into groups. Unless there is outsider repulsion, they can be divided into group clearly and more clearly when high population as shown in Fig. 4.15 (c).
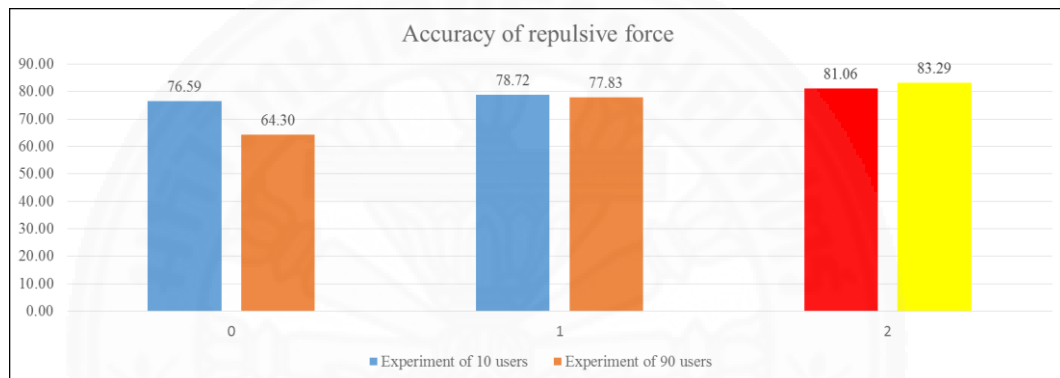
Fig. 4.13 Accuracy of repulsive factor

(a)

(b)

(c)
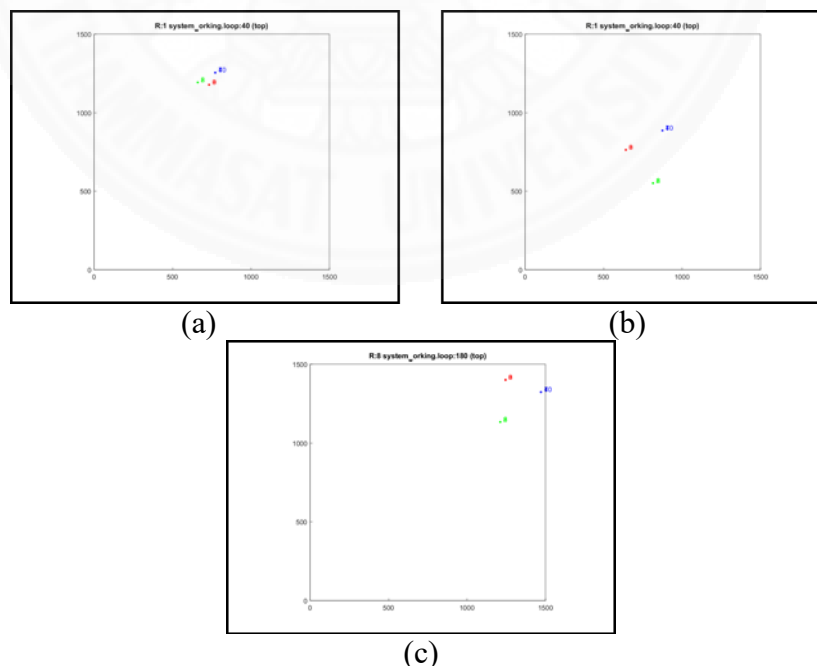
Fig. 4.14 Swarm path display of 10 users, (a) factor 1, (b) factor 2 and (c) factor 3.

41
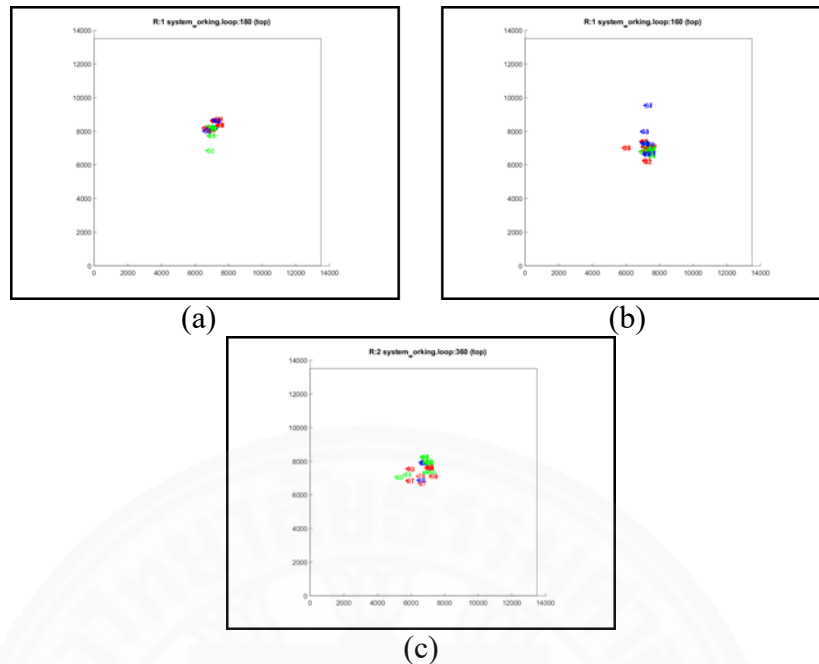
Fig. 4.15 Swarm path display of 90 users, (a) factor 1, (b) factor 2 and (c) factor 3.

In sum, the experimental results of preprocess of PSO present that the best environments of our PSO are follows:

1. Swarming space size equals to 1500 units per dimension for 10 users and equals to 13500 units per dimension for 90 users. Moreover, we can summary that each user have his space, which equals to 150 units per dimension.
2. Maximum radius of neighborhood equals to 200 units.
3. Maximum of velocity has value in range [-50, 50].
4. Repulsive factor equals to 2

All of them are used to examine the human body shape clustering based on PSO in next section.

4.2.2 Experimental result of human body shape clustering based on PSO

The section describes the experimental result of human body shape clustering based on PSO. It consists of a number of cluster graph, table of overall experimental result, 3D body shape groups discussion and the experimental result comparing with k-mean algorithm. We discuss as follows.

42

4.2.2.1 A number of cluster graph
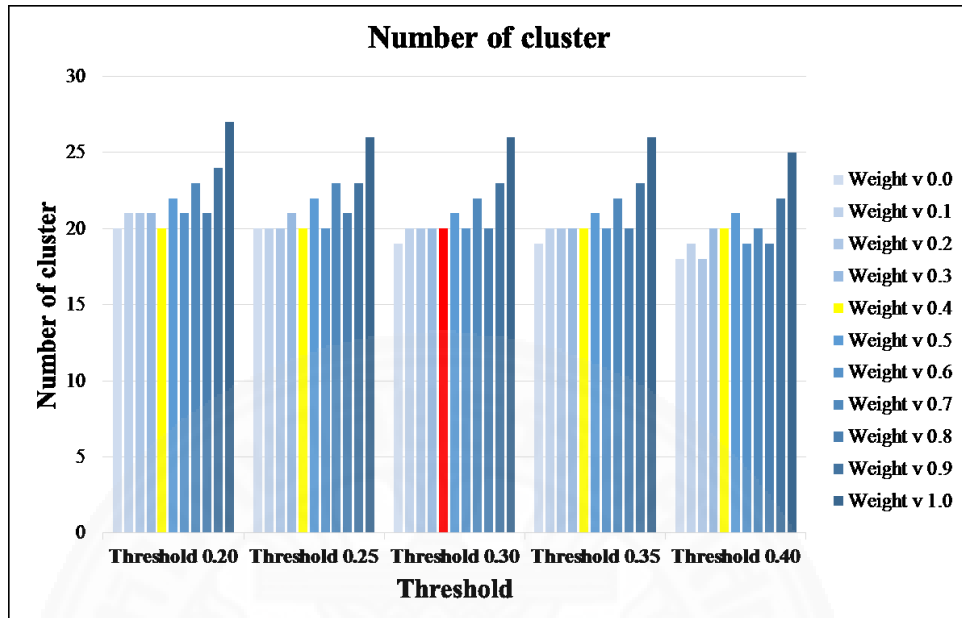
Fig. 4.16 A number of cluster graph

This experiment finds a ratio of fitness function and threshold that are suitable for using in human body shape clustering. A number of cluster graph presents a number of the body shape group that is experimental result between weight of fitness function and threshold. The weight of fitness function is a ratio of volumetric overlap to euclidean distance fitness function. This ration has value from [0: 100] to [100: 0]. For example, [50: 50] is 50 percent of volumetric overlap fitness function and 50 percent of euclidean distance fitness function. It means that system fitness function give equally precedence to both of them. Moreover, threshold is a number that is used to separate friend and outsider. For example, if neighborhood has fitness score less than threshold, he will be assigned as friend. if his fitness score more than threshold, he will be assigned as outsider.

The best ratio as shown in Fig. 4.16 is [40: 60] that is 40 percent of volumetric overlap fitness function and 60 percent of euclidean distance fitness function because after we verified member in the cluster result of each run, it shows that the ratio [40: 60]'s member cluster is the most stable when threshold changing. Moreover, this ratio [40: 60] has not only minimum average iteration but minimum average time as well maximum success rate shown in Table of overall experimental result of the human body shape clustering based on PSO in section 4.2.2.2.

43

4.2.2.2 The overall experimental result of the PSO clustering

Table 4.5 shows that average iteration, success rate and average time in each condition. The minimum average iteration is the ratio [40: 60] of volumetric overlap to euclidean distance fitness function as well as section 4.2.2.1 because this ratio [40: 60] can divide the clearest body shape group in this experiment. Furthermore, the minimum average time conforms minimum average iteration and maximum success rate as well. The success rate is the ratio of the most duplicate result that have same member in each cluster. Those indicators present the best result at threshold 0.3. According to Table 4.5, it shows the overall experimental result of the human body shape clustering based on PSO and it is made more clearly as shown in Fig. 4.17 - 4.19 that is a graph of average iteration, success rate and average time.

Table 4.5 Table of overall experimental result of the human body shape clustering based on PSO

The ratio of volumetric overlap to euclidean distance	Fitness threshold	Average Iteration	Success Rate (%)	Average Time (Sec.)
0:100	0.20	3239.13	60.00	1803.161
	0.25	3010.97	63.33	1743.093
	0.30	2750.43	70.00	1695.236
	0.35	2859.80	66.67	1722.519
	0.40	2940.50	56.67	1696.999
10:90	0.20	3111.57	60.00	1743.184
	0.25	2985.17	70.00	1734.583
	0.30	2613.63	76.67	1605.618
	0.35	2917.00	56.67	1745.725
	0.40	3054.00	50.00	1776.188
20:80	0.20	3120.07	60.00	1754.669
	0.25	2910.93	73.33	1684.425
	0.30	2571.53	76.67	1590.244
	0.35	2918.87	60.00	1753.597
	0.40	3003.10	50.00	1744.800
30:70	0.20	2915.20	70.00	1634.573
	0.25	2710.87	73.33	1631.993
	0.30	2613.37	83.33	1617.554
	0.35	2753.63	70.00	1656.151
	0.40	2990.20	60.00	1725.637
40:60	0.20	2870.23	83.33	1612.120
	0.25	2672.00	90.00	1558.796
	0.30	2501.53	93.33	1549.131
	0.35	2813.47	83.33	1704.956
	0.40	3017.00	66.67	1754.009
50:50	0.20	2832.97	76.67	1577.528
	0.25	2623.57	80.00	1611.640
	0.30	2613.47	86.67	1577.831
	0.35	2819.70	76.67	1704.043

44

	0.40	3050.53	63.33	1751.508
60:40	0.20	2960.77	76.67	1644.969
	0.25	2572.47	83.33	1592.150
	0.30	2621.67	83.33	1622.095
	0.35	2860.23	63.33	1724.390
	0.40	3028.40	53.33	1742.586
70:30	0.20	3037.73	63.33	1697.261
	0.25	2690.00	73.33	1597.639
	0.30	2630.33	86.67	1617.117
	0.35	2838.53	70.00	1712.165
	0.40	3055.57	60.00	1764.831
80:20	0.20	3052.80	56.67	1714.466
	0.25	2814.20	70.00	1633.305
	0.30	2625.07	80.00	1611.236
	0.35	2862.43	73.33	1729.989
	0.40	3050.23	53.33	1760.878
90:10	0.20	3103.00	53.33	1740.886
	0.25	2908.00	63.33	1680.405
	0.30	2634.80	70.00	1622.861
	0.35	2807.80	56.67	1694.205
	0.40	3032.53	53.33	1756.517
100:0	0.20	3084.90	53.33	1720.769
	0.25	2913.67	66.67	1697.802
	0.30	2660.57	73.33	1632.183
	0.35	2890.23	63.33	1738.529
	0.40	3118.83	60.00	1811.180
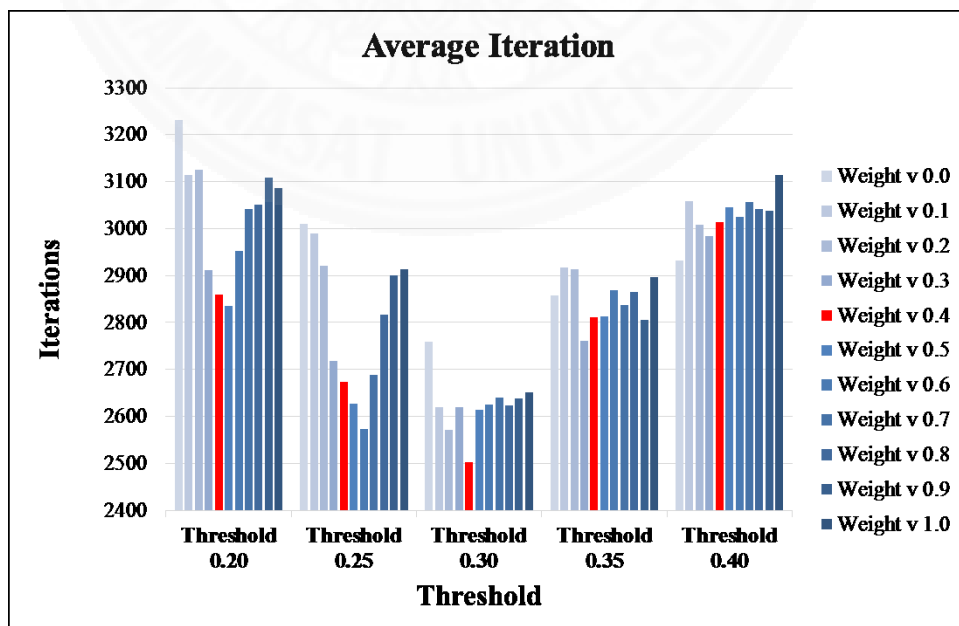
Fig. 4.17 Average Iteration

45
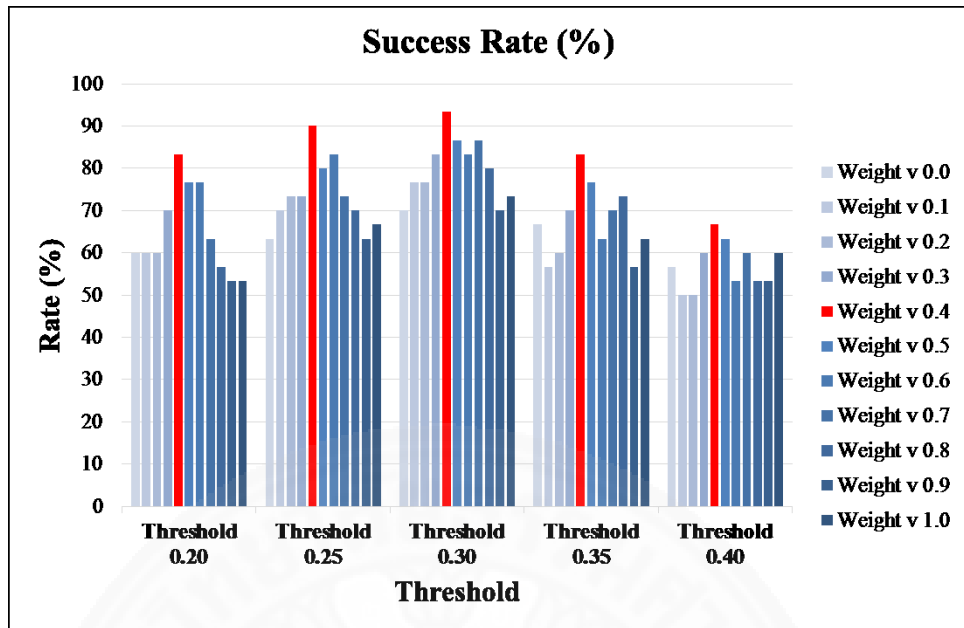
Fig. 4.18 Success Rate
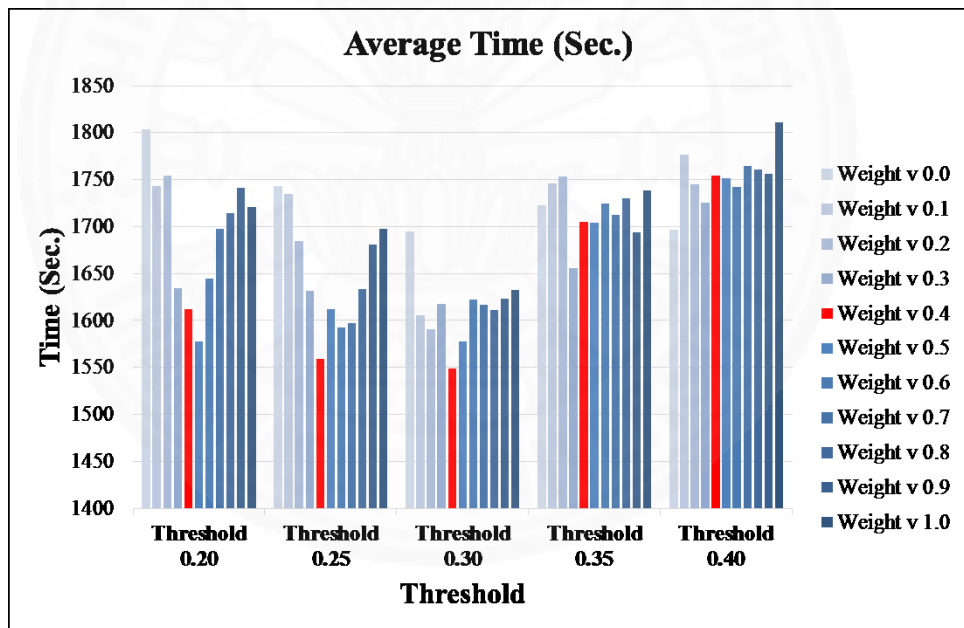
Fig. 4.19 Average Time

The graph of average iteration present that threshold at 0.3 give the minimum average iteration of experimental result when comparing with the other threshold and the graph of average time as well. Moreover, the most important thing is the success rate. The threshold at 0.3 and the ratio [0.4: 0.6] of volumetric overlap to euclidean distance fitness function provides the maximum rate that is 93.33 %.

In sum, by reasoning that confirms the experimental result in section 4.2.2.1 that is a number of cluster graph, we select the experimental result from ratio [0.4: 0.6] and threshold at 0.3 to the best experimental result of the human body shape clustering based on PSO. We discuss it in section 4.2.2.3 as 3D body shape groups discussion part.

46

4.2.2.3 3D body shape groups discussion

In this section, we discuss about 3D body shape groups of the experimental result that is described in section 4.2.2.1 and 4.2.2.2. A number of result group in each body size as follows:

1. Body size 30 has 1 cluster
2. Body size 32 has 2 cluster
3. Body size 34 has 4 cluster
4. Body size 36 has 6 cluster
5. Body size 38 has 3 cluster
6. Body size 40 has 2 cluster
7. Body size 42 has 1 cluster
8. Body size 44 has 1 cluster

A number of groups in each body size present bell curve (a normal distribution), which accords a number of population in each body size of Thai women proposed in [29]. The maximum group of body size is a size 36 in this thesis. Moreover, this size has the most population. Population decrease when it leaves from 50th percentile of the normal distribution. By identifying 3D body shape with FFIT condition [30,31], we can classify the body shape of each body size of the experimental result as shown in Fig. 4.20 - 4.24 and Table 4.6.

Table 4.6 A number of cluster in each body size

Body size	Number of cluster			
	Total	Rectangle shape	Spoon shape	Triangle shape
30	1	1	0	0
32	2	1	0	1
34	4	2	1	1
36	6	3	1	2
38	3	3	0	0
40	2	1	0	1
42	1	1	0	0
44	1	0	0	1

47
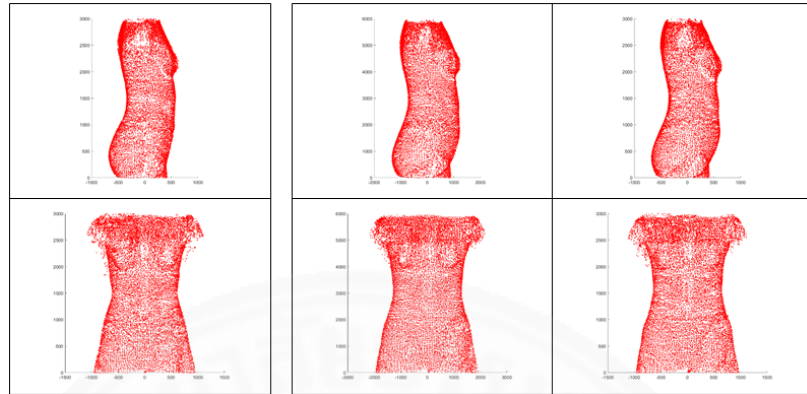
(a)   (b)   (c)

Fig. 4.20 Body size 30 (a) Rectangle shape, size 32 (b) Spoon and (c) Rectangle shape.
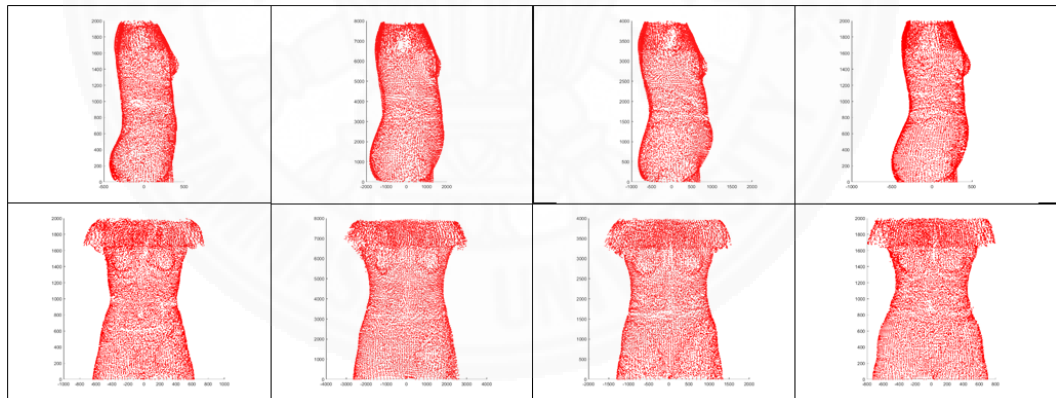
(a)   (b)   (c)   (d)

Fig. 4.21 Body size 34 (a) rectangle shape, (b) rectangle, (c) spoon and (d) triangle shape.
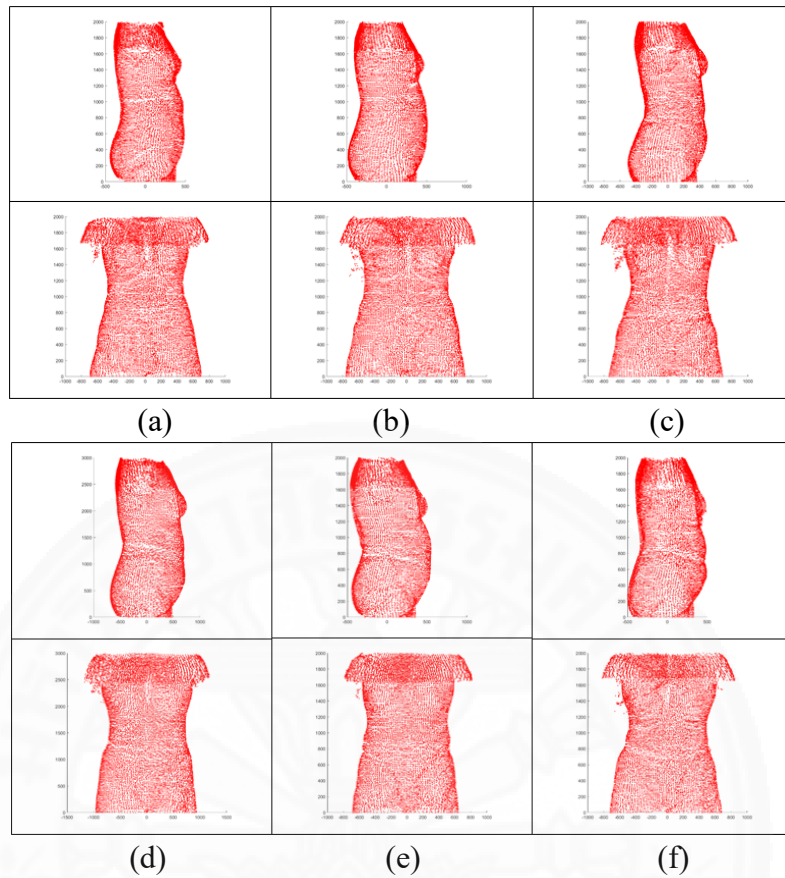
Fig. 4.22 Body size 36 (a) triangle, (b) triangle, (c) spoon, (d) rectangle, (e) rectangle and (f) rectangle shape.
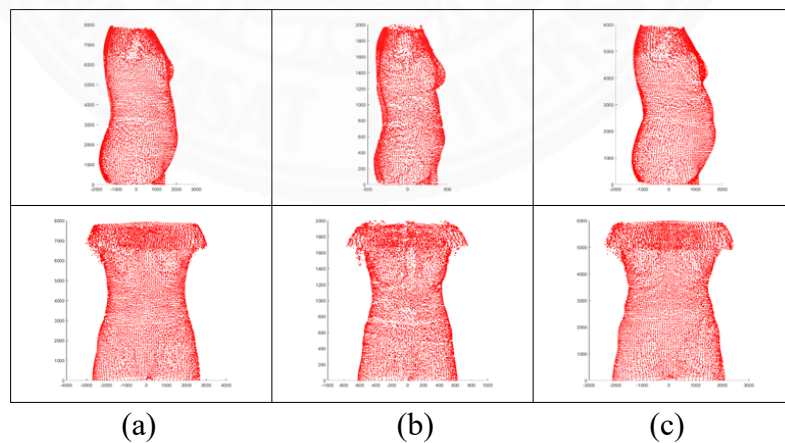
Fig. 4.23 Body size 38 (a) rectangle, (b) rectangle and (c) rectangle shape.
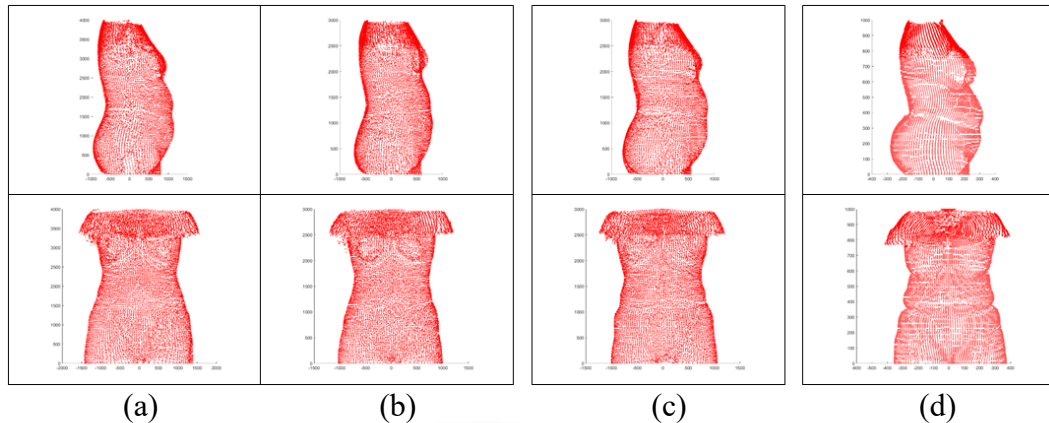
Fig. 4.24 Body size 40 (a) triangle, (b) rectangle shape, size 42 (c) rectangle shape and size 44 (d) triangle shape.

According to Table 4.6, it presents that the clustering based on PSO algorithm can use for clustering 3D human body shape without need of a number of the final group. However, the experimental result shows that some body sizes have duplicate shapes. We check that similarity between these duplicate shapes and then we find that their similarity is more than threshold. It means our fitness function have a limitation because we use volumetric and anthropologic difference. In our view, we can improve the performance of fitness function more than present function. By adding new data to fitness function, they are body landmark height, slope of body edges or information other body landmark, all of which can increase capability of our algorithm in future.

4.2.2.4 The experimental result comparing with k-mean algorithm

This section is the experimental result comparing with a k-mean algorithm in order to compare performance of clustering between both of them. By using a number of groups from PSO result, k-mean algorithm can divide group and then we compare members in each cluster of their results. If outsider mix in same group, this group will be assigned as a failure. Table 4.7 shows that a relationship between each user in body 36 and other users.

Table. 4.7 The relationship between each user in body 36 and other user

User	Body size	Friend	Outsider
1	36	2,3,4,5,6,7,8,10, 11,12,13,14,15, 16,17,19,20,21, 22,24,25,26,	9,18,23,27,28,29,30,31,32,33,34,35,36,37,38,39,40,41,42,43,44, 45,46,47,48,49,50,51,52,53,54,55,56,57,58,59,60,61,62,63,64,65 ,66,67,68,69,70,71,72,73,74,75,76,77,78,79,80,81,82,83,84,85, 86,87,88,89,90,
2	36	1,3,4,5,6,7,8,10, 11,12,13,14,15, 16,17,18,19,20,2	9,23,27,28,29,30,31,32,33,34,35,36,37,38,39,40,41,42,43,44,45, 46,47,48,49,50,51,52,53,54,55,56,57,58,59,60,61,62,63,64,65,66 ,67,68,69,70,71,72,73,74,75,76,77,78,79,80,81,82,83,84,85,86,

		1,22,24,25,26,	87,88,89,90,
3	36	1,2,4,5,6,7,8,10, 11,12,13,14,15, 16,17,18,19,20, 21,22,23,24,25, 26,	9,27,28,29,30,31,32,33,34,35,36,37,38,39,40,41,42,43,44,45,46, 47,48,49,50,51,52,53,54,55,56,57,58,59,60,61,62,63,64,65,66,67 ,68,69,70,71,72,73,74,75,76,77,78,79,80,81,82,83,84,85,86,87, 88,89,90,
4	36	1,2,3,5,6,7,8,10, 11,12,13,14,15, 16,17,18,19,20, 21,22,24,25,26,	9,23,27,28,29,30,31,32,33,34,35,36,37,38,39,40,41,42,43,44,45, 46,47,48,49,50,51,52,53,54,55,56,57,58,59,60,61,62,63,64,65,66 ,67,68,69,70,71,72,73,74,75,76,77,78,79,80,81,82,83,84,85,86, 87,88,89,90,
5	36	1,2,3,4,6,7,8,10, 11,12,13,14,15, 16,17,18,19,20, 21,22,24,25,26,	9,23,27,28,29,30,31,32,33,34,35,36,37,38,39,40,41,42,43,44,45, 46,47,48,49,50,51,52,53,54,55,56,57,58,59,60,61,62,63,64,65,66 ,67,68,69,70,71,72,73,74,75,76,77,78,79,80,81,82,83,84,85,86, 87,88,89,90,
6	36	1,2,3,4,5,7,8,10, 11,12,13,14,15, 16,17,18,19,20, 21,22,23,24,25, 26,	9,27,28,29,30,31,32,33,34,35,36,37,38,39,40,41,42,43,44,45,46, 47,48,49,50,51,52,53,54,55,56,57,58,59,60,61,62,63,64,65,66,67 ,68,69,70,71,72,73,74,75,76,77,78,79,80,81,82,83,84,85,86,87, 88,89,90,
7	36	1,2,3,4,5,6,8,10, 11,12,13,14,15, 16,17,18,19,20, 21,22,24,25,26,	9,23,27,28,29,30,31,32,33,34,35,36,37,38,39,40,41,42,43,44,45, 46,47,48,49,50,51,52,53,54,55,56,57,58,59,60,61,62,63,64,65,66 ,67,68,69,70,71,72,73,74,75,76,77,78,79,80,81,82,83,84,85,86, 87,88,89,90,
8	36	1,2,3,4,5,6,7,10, 11,12,13,14,15, 16,17,18,19,20, 21,22,23,24,25, 26,	9,27,28,29,30,31,32,33,34,35,36,37,38,39,40,41,42,43,44,45,46, 47,48,49,50,51,52,53,54,55,56,57,58,59,60,61,62,63,64,65,66,67 ,68,69,70,71,72,73,74,75,76,77,78,79,80,81,82,83,84,85,86,87, 88,89,90,
9	36	18,23,	1,2,3,4,5,6,7,8,10,11,12,13,14,15,16,17,19,20,21,22,24,25,26,27, 28,29,30,31,32,33,34,35,36,37,38,39,40,41,42,43,44,45,46,47,48 ,49,50,51,52,53,54,55,56,57,58,59,60,61,62,63,64,65,66,67,68, 69,70,71,72,73,74,75,76,77,78,79,80,81,82,83,84,85,86,87,88,89 ,90,
10	36	1,2,3,4,5,6,7,8, 11,12,13,14,15, 16,17,19,20,21, 22,24,25,26,	9,18,23,27,28,29,30,31,32,33,34,35,36,37,38,39,40,41,42,43,44, 45,46,47,48,49,50,51,52,53,54,55,56,57,58,59,60,61,62,63,64,65 ,66,67,68,69,70,71,72,73,74,75,76,77,78,79,80,81,82,83,84,85, 86,87,88,89,90,
11	36	1,2,3,4,5,6,7,8, 10,12,13,14,15, 16,17,18,19,20, 21,22,23,24,25, 26,	9,27,28,29,30,31,32,33,34,35,36,37,38,39,40,41,42,43,44,45,46, 47,48,49,50,51,52,53,54,55,56,57,58,59,60,61,62,63,64,65,66,67 ,68,69,70,71,72,73,74,75,76,77,78,79,80,81,82,83,84,85,86,87, 88,89,90,
12	36	1,2,3,4,5,6,7,8, 10,11,13,14,15, 16,17,18,19,20, 21,22,24,25,26,	9,23,27,28,29,30,31,32,33,34,35,36,37,38,39,40,41,42,43,44,45, 46,47,48,49,50,51,52,53,54,55,56,57,58,59,60,61,62,63,64,65,66 ,67,68,69,70,71,72,73,74,75,76,77,78,79,80,81,82,83,84,85,86, 87,88,89,90,
13	36	1,2,3,4,5,6,7,8, 10,11,12,14,15, 16,17,19,20,21, 22,24,25,26,	9,18,23,27,28,29,30,31,32,33,34,35,36,37,38,39,40,41,42,43,44, 45,46,47,48,49,50,51,52,53,54,55,56,57,58,59,60,61,62,63,64,65 ,66,67,68,69,70,71,72,73,74,75,76,77,78,79,80,81,82,83,84,85, 86,87,88,89,90,
14	36	1,2,3,4,5,6,7,8, 10,11,12,13,15, 16,17,18,19,20, 21,22,24,25,26,	9,23,27,28,29,30,31,32,33,34,35,36,37,38,39,40,41,42,43,44,45, 46,47,48,49,50,51,52,53,54,55,56,57,58,59,60,61,62,63,64,65,66 ,67,68,69,70,71,72,73,74,75,76,77,78,79,80,81,82,83,84,85,86, 87,88,89,90,
15	36	1,2,3,4,5,6,7,8, 10,11,12,13,14,	9,18,23,27,28,29,30,31,32,33,34,35,36,37,38,39,40,41,42,43,44, 45,46,47,48,49,50,51,52,53,54,55,56,57,58,59,60,61,62,63,64,65

51

		16,17,19,20,21, 22,24,25,26,	,66,67,68,69,70,71,72,73,74,75,76,77,78,79,80,81,82,83,84,85, 86,87,88,89,90,
16	36	1,2,3,4,5,6,7,8, 10,11,12,13,14, 15,17,19,20,21, 22,24,25,26,	9,18,23,27,28,29,30,31,32,33,34,35,36,37,38,39,40,41,42,43,44, 45,46,47,48,49,50,51,52,53,54,55,56,57,58,59,60,61,62,63,64,65 ,66,67,68,69,70,71,72,73,74,75,76,77,78,79,80,81,82,83,84,85, 86,87,88,89,90,
17	36	1,2,3,4,5,6,7,8, 10,11,12,13,14, 15,16,18,19,20, 21,22,24,25,26,	9,23,27,28,29,30,31,32,33,34,35,36,37,38,39,40,41,42,43,44,45, 46,47,48,49,50,51,52,53,54,55,56,57,58,59,60,61,62,63,64,65,66 ,67,68,69,70,71,72,73,74,75,76,77,78,79,80,81,82,83,84,85,86, 87,88,89,90,
18	36	2,3,4,5,6,7,8,9, 11,12,14,17,19, 20,23,24,26,	1,10,13,15,16,21,22,25,27,28,29,30,31,32,33,34,35,36,37,38,39, 40,41,42,43,44,45,46,47,48,49,50,51,52,53,54,55,56,57,58,59,60 ,61,62,63,64,65,66,67,68,69,70,71,72,73,74,75,76,77,78,79,80, 81,82,83,84,85,86,87,88,89,90,
19	36	1,2,3,4,5,6,7,8, 10,11,12,13,14, 15,16,17,18,20, 22,23,24,25,26,	9,21,27,28,29,30,31,32,33,34,35,36,37,38,39,40,41,42,43,44,45, 46,47,48,49,50,51,52,53,54,55,56,57,58,59,60,61,62,63,64,65,66 ,67,68,69,70,71,72,73,74,75,76,77,78,79,80,81,82,83,84,85,86, 87,88,89,90,
20	36	1,2,3,4,5,6,7,8, 10,11,12,13,14, 15,16,17,18,19, 21,22,24,25,26,	9,23,27,28,29,30,31,32,33,34,35,36,37,38,39,40,41,42,43,44,45, 46,47,48,49,50,51,52,53,54,55,56,57,58,59,60,61,62,63,64,65,66 ,67,68,69,70,71,72,73,74,75,76,77,78,79,80,81,82,83,84,85,86, 87,88,89,90,
21	36	1,2,3,4,5,6,7,8, 10,11,12,13,14, 15,16,17,20,22, 24,25,26,	9,18,19,23,27,28,29,30,31,32,33,34,35,36,37,38,39,40,41,42,43, 44,45,46,47,48,49,50,51,52,53,54,55,56,57,58,59,60,61,62,63,64 ,65,66,67,68,69,70,71,72,73,74,75,76,77,78,79,80,81,82,83,84, 85,86,87,88,89,90,
22	36	1,2,3,4,5,6,7,8, 10,11,12,13,14, 15,16,17,19,20, 21,24,25,26,	9,18,23,27,28,29,30,31,32,33,34,35,36,37,38,39,40,41,42,43,44, 45,46,47,48,49,50,51,52,53,54,55,56,57,58,59,60,61,62,63,64,65 ,66,67,68,69,70,71,72,73,74,75,76,77,78,79,80,81,82,83,84,85, 86,87,88,89,90,
23	36	3,6,8,9,11,18,19, 24,26,	1,2,4,5,7,10,12,13,14,15,16,17,20,21,22,25,27,28,29,30,31,32,33 ,34,35,36,37,38,39,40,41,42,43,44,45,46,47,48,49,50,51,52,53, 54,55,56,57,58,59,60,61,62,63,64,65,66,67,68,69,70,71,72,73,74 ,75,76,77,78,79,80,81,82,83,84,85,86,87,88,89,90,
24	36	1,2,3,4,5,6,7,8, 10,11,12,13,14, 15,16,17,18,19, 20,21,22,23,25, 26,	9,27,28,29,30,31,32,33,34,35,36,37,38,39,40,41,42,43,44,45,46, 47,48,49,50,51,52,53,54,55,56,57,58,59,60,61,62,63,64,65,66,67 ,68,69,70,71,72,73,74,75,76,77,78,79,80,81,82,83,84,85,86,87, 88,89,90,
25	36	1,2,3,4,5,6,7,8, 10,11,12,13,14, 15,16,17,19,20, 21,22,24,26,	9,18,23,27,28,29,30,31,32,33,34,35,36,37,38,39,40,41,42,43,44, 45,46,47,48,49,50,51,52,53,54,55,56,57,58,59,60,61,62,63,64,65 ,66,67,68,69,70,71,72,73,74,75,76,77,78,79,80,81,82,83,84,85, 86,87,88,89,90,
26	36	1,2,3,4,5,6,7,8, 10,11,12,13,14, 15,16,17,18,19, 20,21,22,23,24, 25,	9,27,28,29,30,31,32,33,34,35,36,37,38,39,40,41,42,43,44,45,46, 47,48,49,50,51,52,53,54,55,56,57,58,59,60,61,62,63,64,65,66,67 ,68,69,70,71,72,73,74,75,76,77,78,79,80,81,82,83,84,85,86,87, 88,89,90,

The experimental result of k-mean algorithm presents that outsider mix in the same group. There are 2 types outsider, such as different body size and same size that his fitness score more than threshold. For example, The experimental result of k-mean algorithm is shown as 16th run.

52

{run:16
    {cluster1: 1, 10, 21, 32, 53, 78 },
    {cluster2: 2, 4, 5, 7, 11, 12, 43, 61, 69, 77 },
    {cluster3: 3, 8, 9, 17, 26, 81 },
    {cluster4: 6, 71, 72, 83 },
    {cluster5: 52 , 57, 58 },
    {cluster6: 13, 15, 16, 22 ,40 ,46 },
    {cluster7: 14 ,20 , 33, 47 ,49 ,55 ,62 ,73 },
    {cluster8: 18 , 67 },
    {cluster9: 19, 66, 76, 84 ,87 },
    {cluster10: 23, 90 },
    {cluster11: 24, 48, 75 },
    {cluster12: 25, 50, 59 },
    {cluster13: 27, 30, 35, 41, 42 },
    {cluster14: 28, 29, 31, 36, 39, 56, 60 },
    {cluster15: 34, 38, 44, 45, 51, 54 ,63 },
    {cluster16: 37, 80 },
    {cluster17: 64, 79 },
    {cluster18: 65, 74, 89 } ,
    {cluster19: 68, 70, 82, 85, 86 },
    {cluster20: 88 }
}

According to 16th k-mean run, cluster1 (1st cluster) has different body size of outsiders that are a group of {1,10,21} (body size 36) and a group of {32,53,78} (other body size). Moreover, cluster3 (3rd cluster) has another outsider that has fitness score more than threshold between a group of {3,8,17,26} and {9}. Furthermore, by comparing result with FFIT condition identifying, the experimental result of our PSO algorithm can be classified 100% or 20 cluster as shown in the previous section (section 4.2.2.3). However, the experimental result of k-mean algorithm can be identified only 80% or 18 cluster. The unidentified cluster are cluster1, 2, 7 and 15 because the identified shape of FFIT condition does not accord with experts. These unidentified clusters are shown in Fig. 4.25.

| (a) | (b) | (c) | (d) |
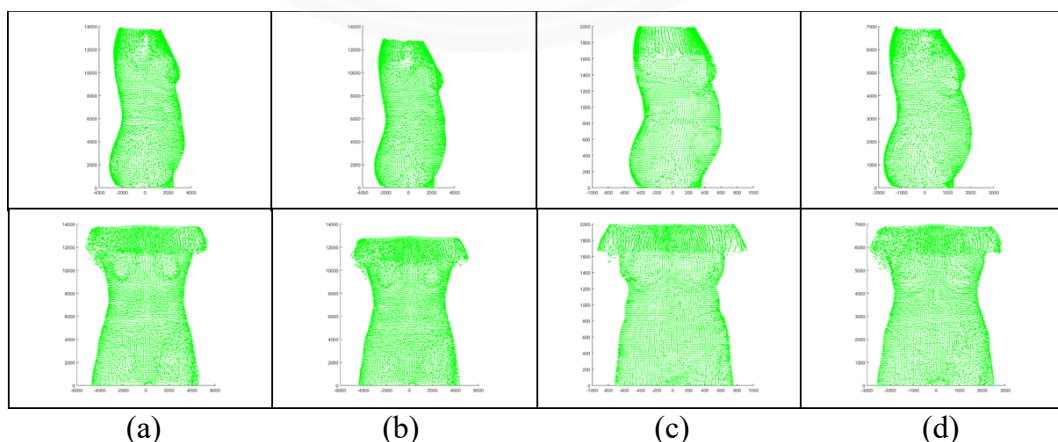
Fig. 4.25 The unidentified cluster (a) cluster 1, (b) cluster 2, (c) cluster 7 and (d) cluster 15.

53

In sum, the human body shape clustering based on PSO algorithm can divide groups of body shape without need to fix a number of the final group. The best condition is threshold at 0.3 and the ratio at [0.4: 0.6] of volumetric overlap to euclidean distance fitness function, which provide the maximum success rate at 93.33 %. Moreover, the best environment of PSO algorithm is follows:

1. Swarming space size equals to 1500 units per dimension for 10 users and equals to 13500 units per dimension for 90 users. Moreover, we can summary that each user have his space, which equals to 150 units per dimension.
2. Maximum radius of neighborhood equals to 200 units.
3. Maximum of velocity has value in range [-50, 50].
4. Repulsive factor equals to 2.

Chapter 5

Conclusions and Future work

The human body shape clustering based on PSO is essential important for reducing updating database time. In this thesis, we implement two methods that are human body analysis and human body shape clustering algorithm. Their details of conclusion are describes following.

5.1 Summary of human body analysis

This thesis presents a human body analysis method that is data acquisition part in this thesis. The purpose of this method is 3D torso data acquisition without depending on the software of 3D scanner. The accuracy of this experimental result is high enough to use as input data for human body shape clustering part. For example, accuracy of bust detection is 100.00%, accuracy of hip detection is 98.89% and accuracy of small of back waist detection is 96.67 %.

In the future work, we will improve the performance of this method in order to detect other body landmarks, such as slope of body edges. Moreover, we will improve the performance of our present work so as to increase their accuracy.

5.2 Summary of human body shape clustering

This method is proposed in order to divide groups of body shapes without training, model recognizing and fixing a number of the final group. It is the clustering based on PSO algorithm. Moreover, we contribute new attributes to it as follows:

1. The fitness function for solving a 3D human body shape clustering problem.
2. The best environment of PSO for solving our problem.
3. An update of assembly point by using the point at previous round.
4. No need to fix a number of maximum friend.
5. A number of maximum round of run that has converged.

Additionally, the experimental results of preprocess of PSO are following:
1. Swarming space size equals to 1500 units per dimension for 10 users and equals to 13500 units per dimension for 90 users. Moreover, we can summary that each user have his space, which equals to 150 units per dimension.
2. Maximum radius of neighborhood equals to 200 units.
3. Maximum of velocity has value in range [-50, 50].
4. Repulsive factor equals to 2.

Finally, the experimental result of human body shape clustering based on PSO algorithm presents that the best result is provided by this condition, which is threshold at 0.3 and the ratio at [0.4: 0.6] of volumetric overlap to euclidean distance fitness function. Not only is its success rate 93.33% but also its average iteration and time is minimum of all conditions. Moreover, the clustering result of PSO and k-mean algorithm comparing presents that the clustering result of PSO algorithm can be identified body shape with FFIT condition at 100.00% or all of 20 clusters but the clustering result of k-mean algorithm can be identified body shape 80.00% or 16 in 20 clusters only.

However, we can improve the performance of our fitness function. By adding new data to fitness function, they are body landmark height, slope of body edges or information other body landmark, all of which can increase capability of our algorithm in future.
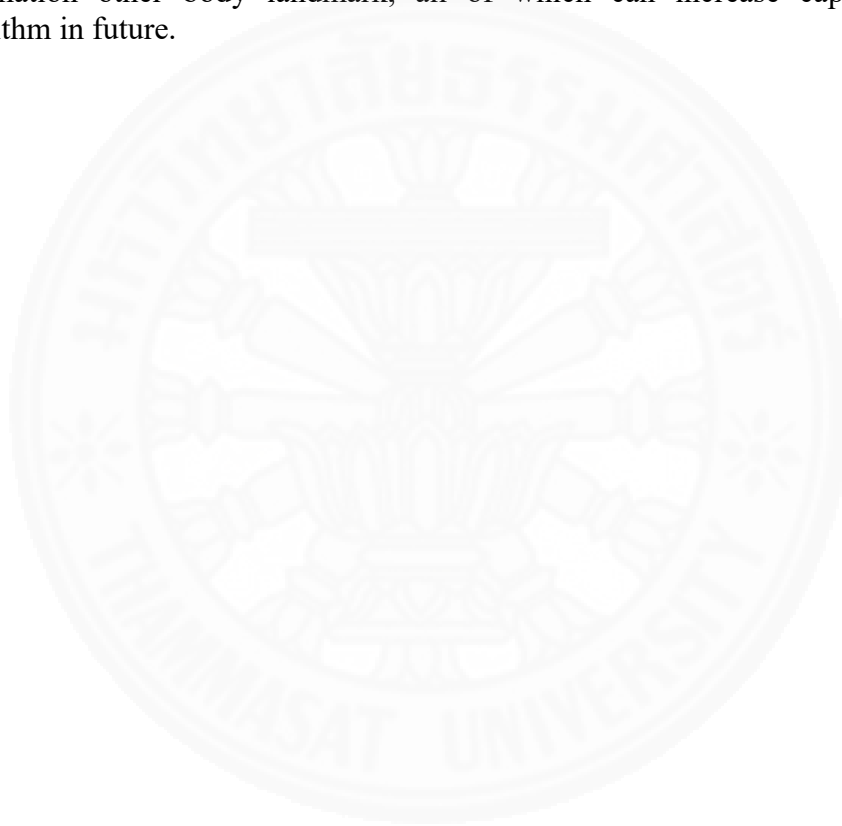
References

[1]   S. Charoensiriwath, "A real-time data monitoring and management system for Thailand's first national sizing survey", in Proc. Portland International Conference on Management of Engineering & Technology (PICMET'08-2008). IEEE, 2008, pp. 856-863.

[2]   S. Charoensiriwath and P. Spichaikul, "Constructing Thailand's national anthropometrics database using 3d body scanning technology", in Proc. the Pacific Neighborhood Consortium Conference, Taipei, Taiwan, 2008.

[3]   Treleaven, P. and Wells, J. "3D Body Scanning and Healthcare Applications" in *IEEE Computer Society*, Vol. 40, No. 7, pp. 28-34, July 2007.

[4]   Bougourd, J. and Treleaven, P., 2010, October. UK National Sizing Survey–SizeUK. In *Proceedings of the International Conference on 3D Body Scanning Technologies, Lugano, Switzerland* (pp. 19-20).

[5]   Size USA. (2005). *Size USA.* Retrieved April 19, 2017, http://www.tc2.com/size-usa.html

[6]   Size KOREA. (2011). *Size Korea.* Retrieved April 19, 2017, https://sizekorea.kr/

[7]   Size-JPN. (2011). *Size Japan.* Retrieved April 19, 2017, http://www.hql.jp/database/size2004/

[8]   Charoensiriwath, Supiya, and P. Spichaikul. "Constructing Thailand's national anthropometrics database using 3d body scanning technology." In *Proc of the Pacific Neighborhood Consortium Conference*. 2009.

[9]   P. Sarakon, Th. Charoenpong, and S. Charoensiriwath, "Face shape classification from 3D human data by using SVM," Int. Conf. of Biomedical Engineering, pp. 1-5, Japan, Nov, 2014.

[10]   P. Sarakon, "3D Face and Body Shape Classification," Unpublished bachelor thesis, Srinakharinwirot University, Nakhonnayok, Thailand, 2014.

[11]   P. Sarakon, S. Charoensiriwath, B. Uyyanonvara and H. Kaneko, "3D body shape clustering based on PSO by multi-fitness function." In *Knowledge and Smart Technology (KST), 2017 9th International Conference on*, pp. 34-39. IEEE, 2017.

[12] A.R. Maria, and C. Mihai, "3D shape recognition software used for classification of the human bodies", 2010 5th Int. Conf. on Virtual Learning (ICVL2010), 2010.

[13] P. Xi, H. Guo and C. Shu, "Human body shape prediction and analysis using predictive clustering tree," Int. Conf. on 3D Imaging, Modeling, Processing, Visualization and Transmission. IEEE, pp: 196-203, 2011.

[14] J. Domingo, M. V. Ibanez, A. Simo, E. Dura, G. Ayala, and S. Aleman, "Modeling of female human body shapes for apparel design based on cross mean sets," Int. Journal of Expert Systems with Applications, Vol. 41, No. 14, pp: 6224-6234, 2014.

[15] G. Vinue, A. Simo, and S. Alemany, "The k-means algorithm for 3D shapes with an application to apparel design," The Journal of Advances in Data Analysis and Classification, Vol. 10, No. 1, pp: 103-132, 2014.

[16] Y. Liu, "Fuzzy clustering algorithm based on PSO in body shape analysis," in Proc. Pacific Asia Workshop on Computational Intelligence and Industrial Applications (PACIIA 2009), 2009, Vol. 2, pp: 209-211.

[17] A. Godil and S. Ressler, "Retrieval and clustering from a 3D human database based on body and head shape," Int. Conf. of SAE Digital Human Modeling, 2006.

[18] H. Loffler-Wirth, E. Willscher, P. Ahnert, K. Wirkner, C. Engel, M. Loeffler and et al, "Novel anthropometry based on 3D-bodyscans applied to a large population based cohort," The Journal of Public Library of Science (PloS one), Vol. 11, No. 7, 2016.

[19] F. Cottle, "Statistical human body form classification: Methodology development and application," PhD Thesis, Auburn University, 2012.

[20] P. Sarakon, S. Charoensiriwath, B. Uyyanonvara and H. Kaneko, "3D Body Shape Clustering based on PSO by Volumetric Overlap," Int. Conf. of Biomedical Engineering. (BMEiCON), 2016 9th (pp. 1-5). IEEE.

[21] R.C. Eberhart and J. Kennedy, "A new optimizer using particle swarm theory", in Proc. the sixth international symposium on micro machine and human science, 1995, pp: 39-43, Japan.

[22]   Kennedy, J. (1997, April). The particle swarm: social adaptation of knowledge. In *Evolutionary Computation, 1997., IEEE International Conference on* (pp. 303-308). IEEE.

[23]   Kennedy, J.F., Kennedy, J., Eberhart, R.C. and Shi, Y., (2001). *Swarm intelligence*. Morgan Kaufmann.

[24]   Eberhart, R., Simpson, P. and Dobbins, R., (1996). *Computational intelligence PC tools*. Academic Press Professional, Inc..

[26]   Kennedy, J. and R. Eberhart (1995). Particle Swarm Optimization. In Proceedings of the IEEE International Conference on Neural Networks, Perth, Australia, pp. 1942-1948.

[26]   Eberhart, R. C., & Shi, Y. (2001). Tracking and optimizing dynamic systems with particle swarms. In *Evolutionary Computation, 2001. Proceedings of the 2001 Congress on* (Vol. 1, pp. 94-100). IEEE.

[27]   Blackwell, T. M., & Bentley, P. J. (2002, July). Dynamic search with charged swarms. In *Proceedings of the 4th Annual Conference on Genetic and Evolutionary Computation* (pp. 19-26). Morgan Kaufmann Publishers Inc..

[28]   S. Ujjin, "Improving capabilities of recommender systems using swarm intelligence," PhD Thesis, University College London, London, England, 2004.

[29]   P. Bunporn, P. Tiyanunti and S. Charoensiriwath, "Thai Women's Body Clustering using K-Means Algorithm", Int. Conf. on Computer Science and Software Engineering (JCSSE), May 13 - May 15, 2009 Phuket, Thailand.

[30]   P. Devarajan, and C. L. Istook, "Validation of female figure identi-fication technique (FFIT) for apparel software," The Journal of Textile and Apparel, Technology and Management, Vol. 4, No. 1, pp: 1-23, 2004.

[31]   J. Yim Lee, C.L. Istook, Y. Ja Nam, and S. Mi Park, "Comparison of body shape between USA and Korean women," Int. Journal of Clothing Science and Technology, Vol. 19, No. 5, pp: 374-391, 2007.

Appendices

Appendix A
List of Publication

1. P. Sarakon, S. Charoensiriwath, B. Uyyanonvara and H. Kaneko, "3D Body Shape Clustering based on PSO by Volumetric Overlap," Int. Conf. of Biomedical Engineering. (BMEiCON), 2016 9th (pp. 1-5). IEEE.

2. P. Sarakon, S. Charoensiriwath, B. Uyyanonvara and H. Kaneko, "3D body shape clustering based on PSO by multi-fitness function." In *Knowledge and Smart Technology (KST), 2017 9th International Conference on*, pp. 34-39. IEEE, 2017.